

Supplementary Materials to the paper entitled:

## **Uranium-mediated Thiourea/Urea Conversion on Chelating Ligands**

**Christelle Njiki Noufele <sup>1</sup>, Maximilian Roca Jungfer <sup>2</sup>, Adelheid Hagenbach <sup>1</sup>, Hung Huy Nguyen <sup>3</sup>,  
and Ulrich Abram <sup>1\*</sup>**

<sup>1</sup> Institute of Chemistry and Biochemistry, Freie Universität Berlin, Fabeckstr. 34/36, 14195 Berlin, Germany.

<sup>2</sup> Institute of Organic Chemistry, Ruprecht-Karls Universität Heidelberg, Im Hohenheimer Feld 271, D-69120 Heidelberg, Germany.

<sup>3</sup> Department of Inorganic Chemistry, VNU University of Science, 19 Le Thanh Tong, Hanoi 100000, Vietnam

## Table of content

<b>1. Crystallographic data.....</b>	<b>4</b>
<b>Table S1.</b> Crystallographic data and data collection parameters.....	4
<b>Figure S1.</b> Ellipsoid representation of the structure of (HNEt <sub>3</sub> )[9]. The thermal ellipsoids are set at a 30% probability level. Hydrogen atoms bonding to carbon atoms are omitted for clarity. ....	6
<b>Table S2.</b> Bond lengths (Å) in (HNEt <sub>3</sub> )[9]. ....	6
<b>Table S3.</b> Bond angles (°) in (HNEt <sub>3</sub> )[9]. ....	7
<b>Figure S2.</b> Ellipsoid representation of the structure of (HNEt <sub>3</sub> )[10], also illustrating the disordered parts of the counter ion. The thermal ellipsoids are set at a 30% probability level. Hydrogen atoms are omitted for clarity. ....	10
<b>Table S4.</b> Bond lengths (Å) in (HNEt <sub>3</sub> )[10]. ....	10
<b>Table S5.</b> Bond angles (°) in (HNEt <sub>3</sub> )[10]. ....	11
<b>Figure S3.</b> Ellipsoid representation of the structure of (EtPPh <sub>3</sub> )[11]. The thermal ellipsoids are set at a 30% probability level. Hydrogen atoms are omitted for clarity. ....	13
<b>Table S6.</b> Bond lengths (Å) in (EtPPh <sub>3</sub> )[11]. ....	13
<b>Table S7.</b> Bond angles (°) in (EtPPh <sub>3</sub> )[11]. ....	14
<b>Figure S4.</b> Ellipsoid representation of the complexes contained in the (EtPPh <sub>3</sub> )[(UO <sub>2</sub> ) <sub>3</sub> (L <sup>2Et2</sup> ) <sub>2</sub> (μ <sub>2</sub> -OMe)(μ <sub>3</sub> -O)] <sub>0.9</sub> /[(UO <sub>2</sub> ) <sub>3</sub> (L <sup>Et2</sup> ) <sub>2</sub> (μ <sub>2</sub> -OMe)(μ <sub>3</sub> -O)] <sub>0.1</sub> mixed-crystals. The thermal ellipsoids are set at a 30% probability level. Hydrogen atoms are omitted for clarity. ....	18
<b>Table S8.</b> Bond lengths (Å) in (EtPPh <sub>3</sub> )[(UO <sub>2</sub> ) <sub>3</sub> (L <sup>2Et2</sup> ) <sub>2</sub> (μ <sub>2</sub> -OMe)(μ <sub>3</sub> -O)] <sub>0.9</sub> /[(UO <sub>2</sub> ) <sub>3</sub> (L <sup>Et2</sup> ) <sub>2</sub> (μ <sub>2</sub> -OMe)(μ <sub>3</sub> -O)] <sub>0.1</sub> . ....	18
<b>Table S9.</b> Bond angles (°) in (EtPPh <sub>3</sub> )[(UO <sub>2</sub> ) <sub>3</sub> (L <sup>2Et2</sup> ) <sub>2</sub> (μ <sub>2</sub> -OMe)(μ <sub>3</sub> -O)] <sub>0.9</sub> /[(UO <sub>2</sub> ) <sub>3</sub> (L <sup>Et2</sup> ) <sub>2</sub> (μ <sub>2</sub> -OMe)(μ <sub>3</sub> -O)] <sub>0.1</sub> . ....	19
<b>2. Selected Spectroscopic Data.....</b>	<b>24</b>
<b>Figure S5.</b> IR spectrum (KBr) of (HNEt <sub>3</sub> )[(UO <sub>2</sub> ) <sub>3</sub> (L <sup>2Et2</sup> ) <sub>2</sub> (μ <sub>2</sub> -OH)(μ <sub>3</sub> -O)], (HNEt <sub>3</sub> )[9]. ....	24
<b>Figure S6.</b> <sup>1</sup> H NMR spectra of (HNEt <sub>3</sub> )[(UO <sub>2</sub> ) <sub>3</sub> (L <sup>2Et2</sup> ) <sub>2</sub> (μ <sub>2</sub> -OH)(μ <sub>3</sub> -O)], (HNEt <sub>3</sub> )[9], in DMSO-D <sub>6</sub> . ....	24
<b>Figure S7.</b> <sup>1</sup> H NMR spectra of (HNEt <sub>3</sub> )[(UO <sub>2</sub> ) <sub>3</sub> (L <sup>2Et2</sup> ) <sub>2</sub> (μ <sub>2</sub> -OH)(μ <sub>3</sub> -O)], (HNEt <sub>3</sub> )[9], in CDCl <sub>3</sub> . ....	25
<b>Figure S8.</b> ESI(-) mass spectrum of (HNEt <sub>3</sub> )[(UO <sub>2</sub> ) <sub>3</sub> (L <sup>2Et2</sup> ) <sub>2</sub> (μ <sub>2</sub> -OH)(μ <sub>3</sub> -O)], (HNEt <sub>3</sub> )[9], in CH <sub>2</sub> Cl <sub>2</sub> . ....	25
<b>Figure S9.</b> IR spectrum (KBr) of (HNEt <sub>3</sub> )[(UO <sub>2</sub> ) <sub>3</sub> (L <sup>2Et2</sup> ) <sub>2</sub> (μ <sub>2</sub> -OEt)(μ <sub>3</sub> -O)], (HNEt <sub>3</sub> )[10]. ....	26
<b>Figure S10.</b> <sup>1</sup> H NMR spectra of (HNEt <sub>3</sub> )[(UO <sub>2</sub> ) <sub>3</sub> (L <sup>2Et2</sup> ) <sub>2</sub> (μ <sub>2</sub> -OEt)(μ <sub>3</sub> -O)], (HNEt <sub>3</sub> )[10], in DMSO-D <sub>6</sub> . ....	26

<b>Figure S11.</b> ESI(–) mass spectrum of $(\text{HNEt}_3)[(\text{UO}_2)_3(\text{L}^{2\text{Et}_2})_2(\mu_2\text{-OEt})(\mu_3\text{-O})]$ , $(\text{HNEt}_3)[\mathbf{10}]$ , in $\text{CH}_2\text{Cl}_2$ .	27
<b>Figure S12.</b> IR spectrum (KBr) of $(\text{EtPPh}_3)[(\text{UO}_2)_3(\text{L}^{2\text{Et}_2})_2(\mu_2\text{-OMe})(\mu_3\text{-O})]$ , $(\text{EtPPh}_3)[\mathbf{11}]$ .	27
<b>Figure S13.</b> $^1\text{H}$ NMR spectra of $(\text{EtPPh}_3)[(\text{UO}_2)_3(\text{L}^{2\text{Et}_2})_2(\mu_2\text{-OMe})(\mu_3\text{-O})]$ , $(\text{EtPPh}_3)[\mathbf{11}]$ , in $\text{DMSO-}d_6$ .	28
<b>3. Computational Chemistry</b>	28
<b>Figure S14.</b> Considered hydrolysis reactions of trimetallic uranium complexes and the corresponding uncoordinated pro-ligands. Relative free energy differences for reactions and the hypothetical isomerization from <i>O,O</i> coordination in <b>C</b> to <i>S,S</i> coordination in <b>C'</b> are provided in SI units (gas-phase, standard conditions, B3LYP/LANL2DZ(uranium)+6-311++G**(others) level). Geometries for the ligand structures were optimized at the B3LYP/6-311G level.	29
<b>Figure S15.</b> DFT optimized structure of <b>A<sup>L</sup></b> (see Fig. S14). Hydrogen atoms bonded to carbon atoms are omitted for clarity. B3LYP/6-311G level. Taken from ref [42].	29
<b>Figure S16.</b> DFT optimized structure of <b>B<sup>L</sup></b> (see Fig. S14). Hydrogen atoms bonded to carbon atoms are omitted for clarity. B3LYP/6-311G level.	29
<b>Figure S17.</b> DFT optimized structure of <b>C<sup>L</sup></b> (see Fig. S14). Hydrogen atoms bonded to carbon atoms are omitted for clarity. B3LYP/6-311G level.	30
<b>Figure S18.</b> DFT optimized structure of <b>A</b> (see Fig. S14). Hydrogen atoms are omitted for clarity. B3LYP/LANL2DZ(uranium)+6-311++G**(others) level.	30
<b>Figure S19.</b> DFT optimized structure of <b>B</b> (see Fig. S14). Hydrogen atoms are omitted for clarity. B3LYP/LANL2DZ(uranium)+6-311++G**(others) level.	30
<b>Figure S20.</b> DFT optimized structure of <b>C</b> (see Fig. S14). Hydrogen atoms are omitted for clarity. B3LYP/LANL2DZ(uranium)+6-311++G**(others) level.	30
<b>Figure S21.</b> DFT optimized structure of <b>C'</b> (see Fig. S14). Hydrogen atoms are omitted for clarity. B3LYP/LANL2DZ(uranium)+6-311++G**(others) level.	31
<b>Table S10.</b> Free energies $\Delta G$ obtained by the DFT calculations (gas-phase, standard conditions, B3LYP/LANL2DZ(uranium)+6-311++G**(others) level). Geometries for the ligand structures were optimized at the B3LYP/6-311G level.	31
<b>Table S11.</b> Energies $E$ obtained by the DFT calculations (gas-phase, top: PBE0-GD3BJ/StuttgartRLC(uranium)+def2-TZVPPD(others) level; bottom: B3LYP/LANL2DZ(uranium)+6-311++G**(others) level).	31
<b>Figure S22.</b> DFT-simulated IR frequencies for the $[(\text{UO}_2)_3(\text{L}^{2\text{Et}_2})_2(\mu_2\text{-OMe})(\mu_3\text{-O})]^-$ anion with spectral resolutions of (a) $2\text{ cm}^{-1}$ , (b) $20\text{ cm}^{-1}$ and (c) $30\text{ cm}^{-1}$ . Note that no cation was included in the calculation. Despite the fact that the simulation has been conducted for the optimized gas phase structure, a good agreement is obtained with the frequencies in the experimental spectrum (see Fig. S12).	32
<b>4. References</b>	33

# 1. Crystallographic data

**Table S1.** Crystallographic data and data collection parameters.

	(HNEt <sub>3</sub> )[(UO <sub>2</sub> ) <sub>3</sub> (L <sup>2Et2</sup> ) <sub>2</sub> (μ <sub>2</sub> -OH)(μ <sub>3</sub> -O)] x H <sub>2</sub> O (HNEt <sub>3</sub> )[9] x H <sub>2</sub> O	(HNEt <sub>3</sub> )[(UO <sub>2</sub> ) <sub>3</sub> (L <sup>2Et2</sup> ) <sub>2</sub> (μ <sub>2</sub> -OEt)(μ <sub>3</sub> -O)] x H <sub>2</sub> O (HNEt <sub>3</sub> )[10] x H <sub>2</sub> O
Empirical formula	C <sub>40</sub> H <sub>65</sub> N <sub>11</sub> O <sub>15</sub> S <sub>2</sub> U <sub>3</sub>	C <sub>42</sub> H <sub>68</sub> N <sub>11</sub> O <sub>15</sub> S <sub>2</sub> U <sub>32</sub>
Formula weight	1718.24	1745.28
Temperature/K	203.15	100
Crystal system	Monoclinic	Orthorhombic
Space group	C2/c	Pnma
a/Å	38.356(2)	23.754(5)
b/Å	9.5250(10)	19.292(4)
c/Å	34.782(2)	13.997(3)
α/°	90	90
β/°	110.67(2)	90
γ/°	90	90
Volume/Å <sup>3</sup>	11889(2)	6414(2)
Z	8	4
ρ <sub>calc</sub> / gcm <sup>-3</sup>	1.920	1.807
μ / mm <sup>-1</sup>	8.288	7.683
F(000)	6480.0	3300.0
Crystal size / mm <sup>3</sup>	0.18 × 0.04 × 0.04	0.73 × 0.04 × 0.03
Radiation	MoKα (λ = 0.71073)	MoKα (λ = 0.71073)
2Θ range for data collection/°	9.178 to 49	4.97 to 49
Index ranges	-43 ≤ h ≤ 44, -11 ≤ k ≤ 11, -40 ≤ l ≤ 40	-27 ≤ h ≤ 27, -20 ≤ k ≤ 22, -16 ≤ l ≤ 16
Reflections collected	41286	44176
Independent reflections	9805 [R <sub>int</sub> = 0.0897, R <sub>sigma</sub> = 0.1004]	5467 [R <sub>int</sub> = 0.0842, R <sub>sigma</sub> = 0.0431]
Data/restraints/parameters	9805/21/552	5467/0/257
Goodness-of-fit on F <sup>2</sup>	0.886	1.111
Final R indexes [I ≥ 2σ (I)]	R <sub>1</sub> = 0.0501, wR <sub>2</sub> = 0.0949	R <sub>1</sub> = 0.0709, wR <sub>2</sub> = 0.1554
Final R indexes [all data]	R <sub>1</sub> = 0.0946, wR <sub>2</sub> = 0.1063	R <sub>1</sub> = 0.0912, wR <sub>2</sub> = 0.1704
Largest diff. peak/hole / e Å <sup>-3</sup>	1.66/-1.40	2.98/-2.72
Diffractometer	STOE IPDS T2	Bruker Apex CCD
Remarks	-	A solvent mask was calculated and 48 electrons were found in a volume of 1160 Å <sup>3</sup> in 1 void per unit cell. This is consistent with the presence of 1 H <sub>2</sub> O per formula unit which account for 40 electrons per unit cell.
CCDC access code	2389008	2389009

**Table S1.** Crystallographic data and data collection parameters (continued)

	(EtPPh <sub>3</sub> )[(UO <sub>2</sub> ) <sub>3</sub> (L <sup>2Et2</sup> ) <sub>2</sub> (μ <sub>2</sub> -OMe)(μ <sub>3</sub> -O)], (EtPPh <sub>3</sub> )[ <b>11</b> ]	(EtPPh <sub>3</sub> )[(UO <sub>2</sub> ) <sub>3</sub> (L <sup>2Et2</sup> ) <sub>2</sub> (μ <sub>2</sub> -OMe)(μ <sub>3</sub> -O)] <sub>0.9</sub> [(UO <sub>2</sub> ) <sub>3</sub> (L <sup>1Et2</sup> ) <sub>2</sub> (μ <sub>2</sub> -OMe)(μ <sub>3</sub> -O)] <sub>0.1</sub>
Empirical formula	C <sub>55</sub> H <sub>69</sub> N <sub>10</sub> O <sub>14</sub> PS <sub>2</sub> U <sub>3</sub>	C <sub>55</sub> H <sub>69</sub> O <sub>13.8</sub> N <sub>10</sub> S <sub>2.2</sub> U <sub>3</sub> P
Formula weight	1903.38	1905.59
Temperature/K	203.15	100.14
Crystal system	Monoclinic	Monoclinic
Space group	P2 <sub>1</sub> /c	P2 <sub>1</sub> /c
a/Å	12.7520(10)	12.61(2)
b/Å	18.3410(10))	18.20(3) )
c/Å	28.125(2) )	27.88(5)
α/°	90	90
β/°	103.020(3)	102.99(4)
γ/°	90	90
Volume/Å <sup>3</sup>	6408.9(8)	6238(17)
Z	4	4
ρ <sub>calc</sub> / gcm <sup>-3</sup>	1.973	2.029
μ / mm <sup>-1</sup>	7.721	7.937
F(000)	3616.0	3620.0
Crystal size / mm <sup>3</sup>	0.68 × 0.04 × 0.04	0.48 × 0.1 × 0.05
Radiation	MoKα (λ = 0.71073)	MoKα (λ = 0.71073)
2θ range for data collection/°	9.198 to 48.998	4.476 to 49
Index ranges	-14 ≤ h ≤ 14, -18 ≤ k ≤ 21, -32 ≤ l ≤ 32	-14 ≤ h ≤ 14, -21 ≤ k ≤ 21, -32 ≤ l ≤ 32
Reflections collected	46613	141413
Independent reflections	10577 [R <sub>int</sub> = 0.0741, R <sub>sigma</sub> = 0.0708]	10374 [R <sub>int</sub> = 0.0656, R <sub>sigma</sub> = 0.0255]
Data/restraints/parameters	10577/42/774	10374/0/765
Goodness-of-fit on F <sup>2</sup>	0.864	1.052
Final R indexes [I>=2σ (I)]	R <sub>1</sub> = 0.0355, wR <sub>2</sub> = 0.0600	R <sub>1</sub> = 0.0291, wR <sub>2</sub> = 0.0546
Final R indexes [all data]	R <sub>1</sub> = 0.0682, wR <sub>2</sub> = 0.0661	R <sub>1</sub> = 0.0385, wR <sub>2</sub> = 0.0580
Largest diff. peak/hole / e Å <sup>-3</sup>	0.91/-1.35	1.85/-1.99
Diffractometer	STOE IPDS	Bruker Apex CCD
Remarks	-	Mixed crystal with „90/10 O/S disorder“ in the uranium-coordinated arm of the chelating ligand due to incomplete hydrolysis.
CCDC access code	2389010	Not deposited

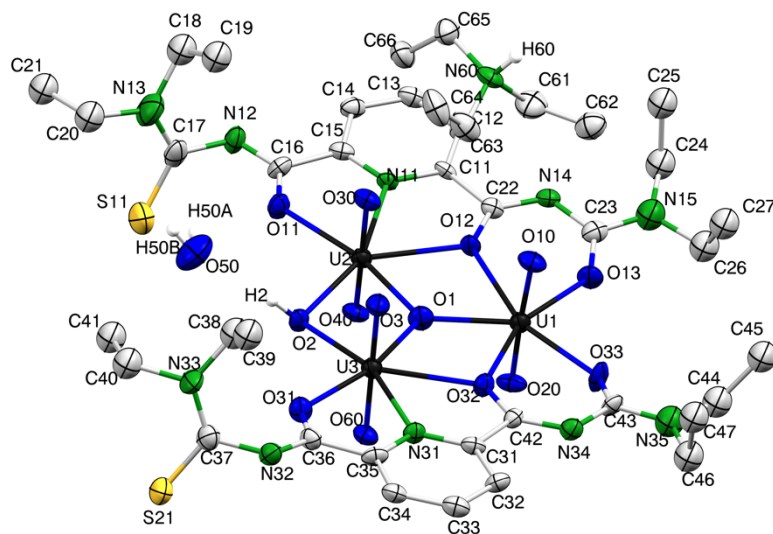


**Figure S1.** Ellipsoid representation of the structure of (HNEt<sub>3</sub>)[9]. The thermal ellipsoids are set at a 30% probability level. Hydrogen atoms bonding to carbon atoms are omitted for clarity.

**Table S2.** Bond lengths (Å) in (HNEt<sub>3</sub>)[9].

U2	U3	3.7352(6)	N13	C18	1.51(2)
U2	U1	3.8760(7)	N34	C43	1.392(15)
U2	O1	2.212(8)	N34	C42	1.304(15)
U2	O40	1.769(8)	N35	C43	1.331(18)
U2	O30	1.773(8)	N35	C46	1.48(2)
U2	O12	2.481(8)	N35	C44	1.47(2)
U2	O2	2.388(8)	N32	C37	1.431(17)
U2	O11	2.345(8)	N32	C36	1.281(15)
U2	N11	2.538(8)	N33	C37	1.342(18)
U3	U1	3.8968(10)	N33	C38	1.47(2)
U3	O1	2.243(8)	N33	C40	1.46(2)
U3	O60	1.777(8)	N11	C11	1.349(14)
U3	O3	1.767(9)	N11	C15	1.343(15)
U3	O2	2.396(7)	N31	C31	1.330(16)
U3	O32	2.486(8)	N31	C35	1.352(15)
U3	O31	2.316(8)	C22	C11	1.504(16)
U3	N31	2.531(9)	C24	C25	1.51(2)
U1	O13	2.340(8)	C26	C27	1.49(2)
U1	O1	2.196(9)	C16	C15	1.494(18)
U1	O12	2.532(7)	C20	C21	1.49(2)
U1	O20	1.774(8)	C18	C19	1.44(2)
U1	O10	1.751(8)	C42	C31	1.502(16)

U1	O33	2.308(8)	C46	C47	1.50(2)
U1	O32	2.507(7)	C44	C45	1.51(2)
S11	C17	1.683(18)	C36	C35	1.480(18)
S21	C37	1.673(16)	C38	C39	1.42(2)
O13	C23	1.257(14)	C40	C41	1.50(2)
O12	C22	1.284(13)	C11	C12	1.385(14)
O11	C16	1.286(14)	C12	C13	1.395(17)
O33	C43	1.242(13)	C13	C14	1.374(19)
O32	C42	1.305(13)	C14	C15	1.399(16)
O31	C36	1.287(13)	C31	C32	1.433(16)
N14	C23	1.379(16)	C32	C33	1.393(17)
N14	C22	1.298(15)	C33	C34	1.387(19)
N15	C23	1.342(19)	C34	C35	1.398(16)
N15	C24	1.50(2)	N60	C61	1.57(2)
N15	C26	1.45(2)	N60	C63	1.446(17)
N12	C17	1.411(18)	N60	C65	1.484(17)
N12	C16	1.280(15)	C61	C62	1.43(2)
N13	C17	1.32(2)	C63	C64	1.53(2)
N13	C20	1.46(2)	C65	C66	1.50(2)

**Table S3.** Bond angles (°) in (HNEt<sub>3</sub>)[9].

U3	U2	U1	61.56(2)	O33	U1	U2	164.0(2)
O1	U2	U3	33.3(2)	O33	U1	U3	106.7(2)
O1	U2	U1	28.3(2)	O33	U1	O13	89.4(3)
O1	U2	O12	68.2(3)	O33	U1	O12	157.1(3)
O1	U2	O2	71.3(3)	O33	U1	O32	68.3(3)
O1	U2	O11	165.1(3)	O32	U1	U2	95.92(18)
O1	U2	N11	130.7(3)	O32	U1	U3	38.52(18)
O40	U2	U3	97.3(3)	O32	U1	O12	134.4(3)
O40	U2	U1	90.1(3)	C23	O13	U1	139.9(9)
O40	U2	O1	92.5(4)	U2	O1	U3	114.0(4)
O40	U2	O30	176.1(4)	U1	O1	U2	123.1(4)
O40	U2	O12	88.4(4)	U1	O1	U3	122.8(4)
O40	U2	O2	90.2(3)	U2	O12	U1	101.3(3)
O40	U2	O11	88.7(4)	C22	O12	U2	126.4(7)
O40	U2	N11	86.6(3)	C22	O12	U1	132.3(8)
O30	U2	U3	86.6(3)	U2	O2	U3	102.6(3)
O30	U2	U1	91.9(3)	C16	O11	U2	127.5(8)
O30	U2	O1	90.8(4)	C43	O33	U1	142.1(8)
O30	U2	O12	90.9(4)	U3	O32	U1	102.6(3)
O30	U2	O2	92.8(3)	C42	O32	U3	126.1(7)
O30	U2	O11	88.7(4)	C42	O32	U1	131.3(7)

O30	U2	N11	89.6(3)	C36	O31	U3	127.8(8)
O12	U2	U3	101.23(16)	C22	N14	C23	119.5(10)
O12	U2	U1	39.83(16)	C23	N15	C24	122.2(14)
O12	U2	N11	62.6(3)	C23	N15	C26	121.0(14)
O2	U2	U3	38.75(18)	C26	N15	C24	116.8(15)
O2	U2	U1	99.52(18)	C16	N12	C17	117.8(11)
O2	U2	O12	139.3(2)	C17	N13	C20	121.8(17)
O2	U2	N11	157.9(3)	C17	N13	C18	121.2(15)
O11	U2	U3	131.9(2)	C20	N13	C18	117.0(15)
O11	U2	U1	166.6(2)	C42	N34	C43	119.7(10)
O11	U2	O12	126.8(3)	C43	N35	C46	122.1(14)
O11	U2	O2	93.8(3)	C43	N35	C44	119.7(13)
O11	U2	N11	64.2(3)	C44	N35	C46	118.1(14)
N11	U2	U3	163.3(2)	C36	N32	C37	119.3(11)
N11	U2	U1	102.4(2)	C37	N33	C38	123.7(13)
U2	U3	U1	60.999(16)	C37	N33	C40	120.1(14)
O1	U3	U2	32.8(2)	C40	N33	C38	115.8(14)
O1	U3	U1	28.3(2)	C11	N11	U2	121.6(7)
O1	U3	O2	70.6(3)	C15	N11	U2	118.4(7)
O1	U3	O32	67.2(3)	C15	N11	C11	120.0(9)
O1	U3	O31	166.2(3)	C31	N31	U3	122.1(7)
O1	U3	N31	129.6(3)	C31	N31	C35	119.7(10)
O60	U3	U2	96.0(2)	C35	N31	U3	118.2(8)
O60	U3	U1	90.3(3)	O13	C23	N14	127.6(13)
O60	U3	O1	92.0(4)	O13	C23	N15	118.1(13)
O60	U3	O2	88.6(3)	N15	C23	N14	114.2(12)
O60	U3	O32	88.0(3)	O12	C22	N14	130.8(11)
O60	U3	O31	88.5(3)	O12	C22	C11	114.7(10)
O60	U3	N31	88.8(3)	N14	C22	C11	114.5(10)
O3	U3	U2	88.0(3)	N15	C24	C25	111.1(14)
O3	U3	U1	92.0(3)	N15	C26	C27	112.1(15)
O3	U3	O1	91.6(4)	N12	C17	S11	119.8(13)
O3	U3	O60	176.1(4)	N13	C17	S11	125.0(13)
O3	U3	O2	94.2(4)	N13	C17	N12	114.9(15)
O3	U3	O32	91.8(4)	O11	C16	C15	115.1(11)
O3	U3	O31	88.4(4)	N12	C16	O11	128.1(13)
O3	U3	N31	87.6(4)	N12	C16	C15	116.7(11)
O2	U3	U2	38.6(2)	N13	C20	C21	110.1(14)
O2	U3	U1	98.8(2)	C19	C18	N13	105.8(15)
O2	U3	O32	137.5(3)	O33	C43	N34	126.1(11)
O2	U3	N31	159.7(3)	O33	C43	N35	119.6(12)
O32	U3	U2	99.86(16)	N35	C43	N34	113.9(11)
O32	U3	U1	38.90(16)	O32	C42	C31	113.6(10)



O32	U3	N31	62.5(3)	N34	C42	O32	130.7(11)
O31	U3	U2	133.5(2)	N34	C42	C31	115.6(10)
O31	U3	U1	165.5(2)	N35	C46	C47	112.8(15)
O31	U3	O2	95.6(3)	N35	C44	C45	114.6(15)
O31	U3	O32	126.6(3)	N32	C37	S21	118.1(11)
O31	U3	N31	64.2(3)	N33	C37	S21	125.2(12)
N31	U3	U2	161.6(2)	N33	C37	N32	116.5(13)
N31	U3	U1	101.3(2)	O31	C36	C35	115.3(10)
U2	U1	U3	57.442(13)	N32	C36	O31	126.2(12)
O13	U1	U2	106.5(2)	N32	C36	C35	118.5(11)
O13	U1	U3	163.9(2)	C39	C38	N33	110.6(15)
O13	U1	O12	67.7(3)	N33	C40	C41	112.1(14)
O13	U1	O32	157.4(3)	N11	C11	C22	114.8(9)
O1	U1	U2	28.6(2)	N11	C11	C12	121.7(10)
O1	U1	U3	28.9(2)	C12	C11	C22	123.4(11)
O1	U1	O13	135.0(3)	C11	C12	C13	117.7(12)
O1	U1	O12	67.4(3)	C14	C13	C12	121.0(11)
O1	U1	O33	135.5(3)	C13	C14	C15	118.0(12)
O1	U1	O32	67.5(3)	N11	C15	C16	114.6(10)
O12	U1	U2	38.87(18)	N11	C15	C14	121.4(12)
O12	U1	U3	96.16(18)	C14	C15	C16	124.0(12)
O20	U1	U2	91.0(3)	N31	C31	C42	115.8(10)
O20	U1	U3	92.1(3)	N31	C31	C32	122.4(11)
O20	U1	O13	88.8(4)	C32	C31	C42	121.8(12)
O20	U1	O1	90.2(4)	C33	C32	C31	116.7(13)
O20	U1	O12	93.2(3)	C34	C33	C32	120.8(12)
O20	U1	O33	88.1(4)	C33	C34	C35	118.5(12)
O20	U1	O32	93.6(3)	N31	C35	C36	113.9(10)
O10	U1	U2	90.8(3)	N31	C35	C34	121.8(12)
O10	U1	U3	91.0(3)	C34	C35	C36	124.3(12)
O10	U1	O13	88.2(4)	C63	N60	C61	108.8(12)
O10	U1	O1	92.5(4)	C63	N60	C65	118.1(13)
O10	U1	O12	86.6(3)	C65	N60	C61	110.2(11)
O10	U1	O20	176.9(4)	C62	C61	N60	117.7(13)
O10	U1	O33	91.0(4)	N60	C63	C64	114.9(15)
O10	U1	O32	88.8(3)	N60	C65	C66	116.6(13)

---

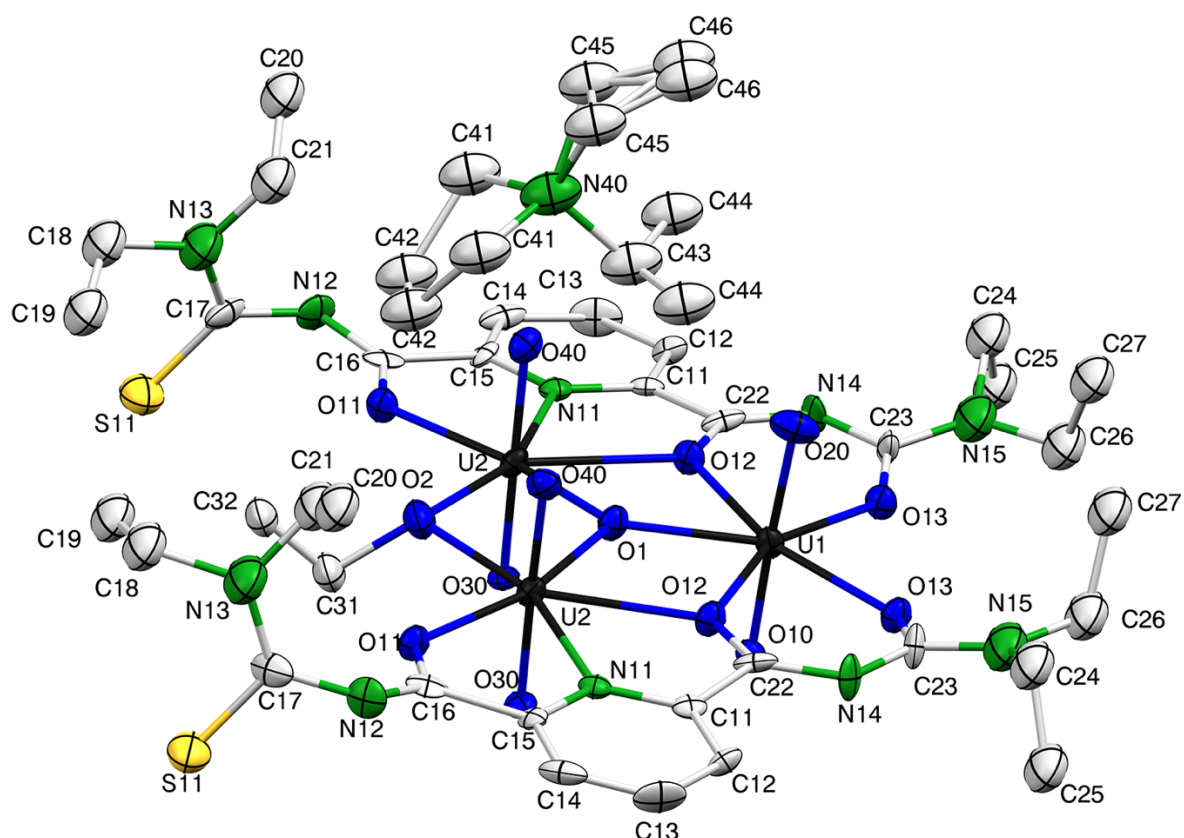


**Figure S2.** Ellipsoid representation of the structure of (HNEt<sub>3</sub>)[10], also illustrating the disordered parts of the counter ion. The thermal ellipsoids are set at a 30% probability level. Hydrogen atoms are omitted for clarity.

**Table S4.** Bond lengths (Å) in (HNEt<sub>3</sub>)[10].

U2	U21	3.7396(13)	C15	C14	1.37(2)
U2	U1	3.9193(11)	N12	C16	1.27(2)
U2	O12	2.510(11)	N12	C17	1.38(2)
U2	O1	2.252(8)	C11	C12	1.39(2)
U2	O40	1.778(11)	C12	C13	1.38(2)
U2	O30	1.805(10)	C23	N15	1.32(2)
U2	O11	2.341(11)	N15	C26	1.45(3)
U2	N11	2.560(12)	N15	C24	1.58(3)
U2	O2	2.361(10)	C13	C14	1.38(3)
U1	O121	2.535(10)	C17	N13	1.34(3)
U1	O12	2.535(10)	N13	C18	1.48(3)
U1	O1	2.205(15)	N13	C21	1.46(3)
U1	O20	1.847(17)	C26	C27	1.49(3)
U1	O10	1.781(15)	C25	C24	1.44(3)
U1	O13	2.342(10)	C18	C19	1.48(3)
U1	O131	2.342(10)	C21	C20	1.42(3)
S11	C17	1.701(19)	O2	C31	1.48(3)
O12	C22	1.290(18)	C31	C32	1.30(4)
O11	C16	1.297(19)	N40	C43	1.59(5)

O13	C23	1.265(18)	N40	C41	1.58(6)
N11	C15	1.336(18)	N40	C45	1.63(5)
N11	C11	1.34(2)	C43	C441	1.46(5)
N14	C22	1.33(2)	C43	C44	1.46(5)
N14	C23	1.35(2)	C41	C42	1.65(7)
C22	C11	1.51(2)	C46	C45	1.41(6)
C15	C16	1.56(2)			

<sup>1</sup> x, 1/2-y, z

**Table S5.** Bond angles (°) in (HNEt<sub>3</sub>)[10].

U2 <sup>1</sup>	U2	U1	61.506(12)	O13 <sup>1</sup>	U1	U2 <sup>1</sup>	107.0(3)
O12	U2	U2 <sup>1</sup>	100.8(2)	O13	U1	U2	107.0(3)
O12	U2	U1	39.3(2)	O13	U1	U2 <sup>1</sup>	163.7(3)
O12	U2	N11	62.3(4)	O13	U1	O12	68.3(3)
O1	U2	U2 <sup>1</sup>	33.9(3)	O13	U1	O12 <sup>1</sup>	156.9(3)
O1	U2	U1	28.1(3)	O13 <sup>1</sup>	U1	O12 <sup>1</sup>	68.3(3)
O1	U2	O12	67.2(4)	O13 <sup>1</sup>	U1	O12	156.9(3)
O1	U2	O11	165.9(4)	O13	U1	O13 <sup>1</sup>	88.7(5)
O1	U2	N11	129.4(4)	U2	O12	U1	101.9(4)
O1	U2	O2	71.3(5)	C22	O12	U2	126.4(10)
O40	U2	U2 <sup>1</sup>	94.7(3)	C22	O12	U1	131.6(10)
O40	U2	U1	92.8(3)	U2	O1	U2 <sup>1</sup>	112.3(6)
O40	U2	O12	89.6(4)	U1	O1	U2	123.2(3)
O40	U2	O1	90.4(5)	U1	O1	U2 <sup>1</sup>	123.2(3)
O40	U2	O30	176.2(5)	C16	O11	U2	128.0(11)
O40	U2	O11	88.3(4)	C23	O13	U1	139.8(10)
O40	U2	N11	88.4(4)	C15	N11	U2	119.2(10)
O40	U2	O2	93.0(6)	C15	N11	C11	119.6(13)
O30	U2	U2 <sup>1</sup>	89.0(3)	C11	N11	U2	121.2(10)
O30	U2	U1	88.3(3)	C22	N14	C23	121.5(13)
O30	U2	O12	88.9(4)	O12	C22	N14	129.6(14)
O30	U2	O1	92.3(5)	O12	C22	C11	113.6(14)
O30	U2	O11	89.8(4)	N14	C22	C11	116.7(13)
O30	U2	N11	87.9(4)	N11	C15	C16	113.3(13)
O30	U2	O2	90.5(5)	N11	C15	C14	121.4(15)
O11	U2	U2 <sup>1</sup>	132.4(2)	C14	C15	C16	125.3(14)
O11	U2	U1	166.0(2)	C16	N12	C17	119.5(15)
O11	U2	O12	126.8(3)	N11	C11	C22	116.2(13)
O11	U2	N11	64.6(4)	N11	C11	C12	121.8(14)
O11	U2	O2	94.8(4)	C12	C11	C22	122.0(14)
N11	U2	U2 <sup>1</sup>	162.8(3)	C13	C12	C11	118.4(15)
N11	U2	U1	101.5(3)	O13	C23	N14	126.5(14)

O2	U2	U2 <sup>1</sup>	37.6(3)	O13	C23	N15	118.2(16)
O2	U2	U1	99.1(3)	N15	C23	N14	115.3(16)
O2	U2	O12	138.4(4)	C23	N15	C26	124(2)
O2	U2	N11	159.3(4)	C23	N15	C24	121.1(19)
U2	U1	U2 <sup>1</sup>	56.99(2)	C26	N15	C24	114(2)
O12 <sup>1</sup>	U1	U2	95.8(2)	O11	C16	C15	114.4(14)
O12	U1	U2 <sup>1</sup>	95.8(2)	N12	C16	O11	128.2(17)
O12 <sup>1</sup>	U1	U2 <sup>1</sup>	38.8(2)	N12	C16	C15	117.1(15)
O12	U1	U2	38.8(2)	C14	C13	C12	118.9(15)
O12	U1	O12 <sup>1</sup>	134.6(5)	C15	C14	C13	119.9(15)
O1	U1	U2 <sup>1</sup>	28.75(5)	N12	C17	S11	119.6(13)
O1	U1	U2	28.75(5)	N13	C17	S11	120.8(16)
O1	U1	O12 <sup>1</sup>	67.3(2)	N13	C17	N12	119.5(18)
O1	U1	O12	67.3(2)	C17	N13	C18	122(2)
O1	U1	O13 <sup>1</sup>	135.7(3)	C17	N13	C21	121.7(19)
O1	U1	O13	135.7(3)	C21	N13	C18	116(2)
O20	U1	U2 <sup>1</sup>	94.1(6)	N15	C26	C27	114(2)
O20	U1	U2	94.1(6)	C25	C24	N15	104(2)
O20	U1	O12 <sup>1</sup>	91.8(4)	C19	C18	N13	117(2)
O20	U1	O12	91.8(4)	C20	C21	N13	112(2)
O20	U1	O1	90.7(8)	U2	O2	U2 <sup>1</sup>	104.7(7)
O20	U1	O13 <sup>1</sup>	90.0(5)	C31	O2	U2 <sup>1</sup>	118.3(7)
O20	U1	O13	90.0(5)	C31	O2	U2	118.3(7)
O10	U1	U2 <sup>1</sup>	87.9(4)	C32	C31	O2	103(2)
O10	U1	U2	87.9(4)	C43	N40	C45	112(3)
O10	U1	O12 <sup>1</sup>	89.1(3)	C41	N40	C43	110(3)
O10	U1	O12	89.1(3)	C41	N40	C45	97(3)
O10	U1	O1	91.6(6)	C44 <sup>1</sup>	C43	N40	106(3)
O10	U1	O20	177.7(8)	C44	C43	N40	106(3)
O10	U1	O13 <sup>1</sup>	88.4(4)	C44	C43	C44 <sup>1</sup>	127(5)
O10	U1	O13	88.4(4)	N40	C41	C42	103(3)
O13 <sup>1</sup>	U1	U2	163.7(3)	C46	C45	N40	122(4)

<sup>1</sup> x, 1/2-y, z

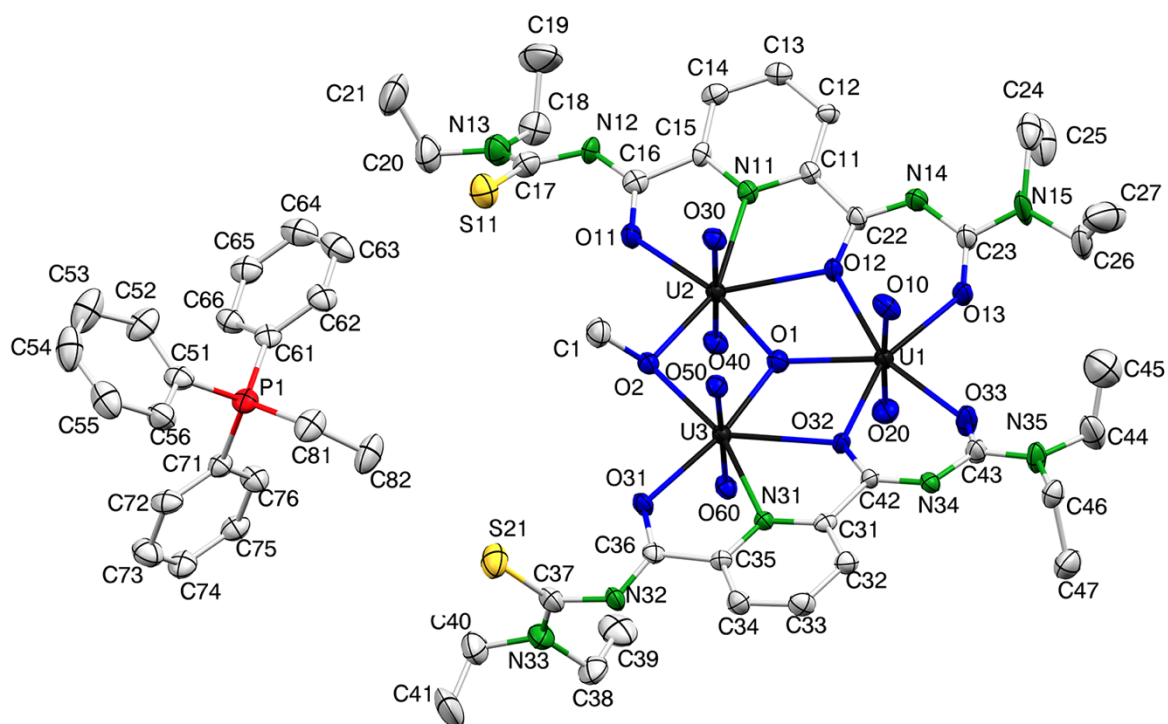


**Figure S3.** Ellipsoid representation of the structure of (EtPPh<sub>3</sub>)[11]. The thermal ellipsoids are set at a 30% probability level. Hydrogen atoms are omitted for clarity.

**Table S6.** Bond lengths (Å) in (EtPPh<sub>3</sub>)[11].

U2	U3	3.7143(5)	N13	C17	1.360(12)
U2	U1	3.8963(5)	N13	C18	1.473(13)
U2	O30	1.767(5)	N13	C20	1.452(12)
U2	O40	1.763(5)	N31	C31	1.336(9)
U2	O2	2.368(5)	N31	C35	1.339(9)
U2	O1	2.225(6)	N11	C11	1.361(9)
U2	O12	2.504(5)	N11	C15	1.327(10)
U2	O11	2.351(5)	C42	C31	1.508(10)
U2	N11	2.542(7)	C44	C45	1.381(18)
U3	U1	3.9029(4)	C46	C47	1.538(13)
U3	O60	1.773(5)	C36	C35	1.509(10)
U3	O32	2.515(4)	C38	C39	1.498(17)
U3	O50	1.774(5)	C40	C41	1.466(18)
U3	O2	2.367(5)	C22	C11	1.472(11)
U3	O1	2.227(6)	C24	C25	1.360(15)
U3	O31	2.349(5)	C16	C15	1.496(11)
U3	N31	2.542(6)	C18	C19	1.472(17)
U1	O33	2.331(6)	C20	C21	1.492(17)
U1	O32	2.492(5)	C31	C32	1.374(11)
U1	O20	1.764(5)	C32	C33	1.394(11)
U1	O10	1.761(5)	C33	C34	1.379(11)

U1	O1	2.202(5)	C34	C35	1.371(11)
U1	O13	2.342(5)	C11	C12	1.391(11)
U1	O12	2.498(5)	C12	C13	1.402(11)
S21	C37	1.682(10)	C13	C14	1.396(11)
S11	C17	1.705(11)	C14	C15	1.390(11)
O33	C43	1.285(10)	P1	C81	1.777(9)
O32	C42	1.283(9)	P1	C71	1.791(8)
O2	C1	1.458(9)	P1	C51	1.787(10)
O31	C36	1.282(9)	P1	C61	1.775(10)
O13	C23	1.259(10)	C81	C82	1.543(12)
O12	C22	1.286(9)	C76	C75	1.389(11)
O11	C16	1.294(10)	C76	C71	1.384(11)
N34	C43	1.365(10)	C75	C74	1.370(13)
N34	C42	1.292(9)	C74	C73	1.375(14)
N35	C43	1.335(10)	C73	C72	1.413(12)
N35	C44	1.544(13)	C72	C71	1.376(12)
N35	C46	1.469(11)	C56	C55	1.419(15)
N32	C37	1.406(10)	C56	C51	1.403(14)
N32	C36	1.289(10)	C55	C54	1.370(18)
N33	C37	1.331(11)	C54	C53	1.357(19)
N33	C38	1.465(12)	C53	C52	1.391(16)
N33	C40	1.490(11)	C52	C51	1.380(14)
N14	C23	1.394(11)	C66	C65	1.377(13)
N14	C22	1.306(9)	C66	C61	1.382(12)
N15	C23	1.325(10)	C65	C64	1.373(14)
N15	C24	1.638(15)	C64	C63	1.385(16)
N15	C26	1.489(12)	C63	C62	1.397(15)
N12	C17	1.369(11)	C62	C61	1.407(12)
N12	C16	1.286(10)	C26	C27	1.45(2)

**Table S7.** Bond angles (°) in (EtPPh<sub>3</sub>)[11].

U3	U2	U1	61.648(8)	C1	O2	U3	119.3(5)
O30	U2	U3	91.54(19)	U2	O1	U3	113.1(2)
O30	U2	U1	91.50(17)	U1	O1	U2	123.3(3)
O30	U2	O2	89.0(2)	U1	O1	U3	123.6(3)
O30	U2	O1	91.5(2)	C36	O31	U3	125.6(5)
O30	U2	O12	89.2(2)	C23	O13	U1	137.5(5)
O30	U2	O11	91.3(2)	U1	O12	U2	102.34(18)
O30	U2	N11	84.1(2)	C22	O12	U2	124.4(5)
O40	U2	U3	90.4(2)	C22	O12	U1	132.4(4)
O40	U2	U1	90.30(18)	C16	O11	U2	126.8(5)
O40	U2	O30	177.8(3)	C42	N34	C43	121.6(7)

O40	U2	O2	91.9(2)	C43	N35	C44	119.2(8)
O40	U2	O1	90.7(2)	C43	N35	C46	122.8(7)
O40	U2	O12	91.4(2)	C46	N35	C44	117.7(7)
O40	U2	O11	86.6(2)	C36	N32	C37	120.5(7)
O40	U2	N11	94.3(2)	C37	N33	C38	122.4(8)
O2	U2	U3	38.32(13)	C37	N33	C40	121.6(9)
O2	U2	U1	99.93(13)	C38	N33	C40	115.9(8)
O2	U2	O12	138.60(18)	C22	N14	C23	121.7(7)
O2	U2	N11	157.88(19)	C23	N15	C24	121.5(8)
O1	U2	U3	33.48(13)	C23	N15	C26	120.4(9)
O1	U2	U1	28.17(13)	C26	N15	C24	117.8(7)
O1	U2	O2	71.77(18)	C16	N12	C17	127.9(8)
O1	U2	O12	66.93(18)	C17	N13	C18	121.8(8)
O1	U2	O11	166.66(19)	C17	N13	C20	121.2(9)
O1	U2	N11	129.25(19)	C20	N13	C18	117.0(9)
O12	U2	U3	100.41(12)	C31	N31	U3	122.2(5)
O12	U2	U1	38.78(12)	C31	N31	C35	119.3(7)
O12	U2	N11	62.50(19)	C35	N31	U3	118.1(5)
O11	U2	U3	133.38(14)	C11	N11	U2	121.2(5)
O11	U2	U1	164.59(14)	C15	N11	U2	118.7(5)
O11	U2	O2	95.25(18)	C15	N11	C11	119.6(7)
O11	U2	O12	126.15(18)	O33	C43	N34	125.3(7)
O11	U2	N11	64.0(2)	O33	C43	N35	118.4(7)
N11	U2	U3	162.30(13)	N35	C43	N34	116.1(8)
N11	U2	U1	101.24(14)	O32	C42	N34	130.2(7)
U2	U3	U1	61.47(18)	O32	C42	C31	114.0(6)
O60	U3	U2	91.14(19)	N34	C42	C31	115.8(7)
O60	U3	U1	88.00(16)	C45	C44	N35	108.2(13)
O60	U3	O32	90.8(2)	N35	C46	C47	109.7(8)
O60	U3	O50	176.5(3)	N32	C37	S21	118.5(7)
O60	U3	O2	94.3(2)	N33	C37	S21	125.3(7)
O60	U3	O1	89.6(2)	N33	C37	N32	115.8(8)
O60	U3	O31	86.6(2)	O31	C36	N32	128.7(7)
O60	U3	N31	92.1(2)	O31	C36	C35	116.7(7)
O32	U3	U2	99.85(12)	N32	C36	C35	114.5(8)
O32	U3	U1	38.57(12)	N33	C38	C39	110.3(10)
O32	U3	N31	61.71(17)	C41	C40	N33	110.0(11)
O50	U3	U2	92.33(18)	O13	C23	N14	126.6(7)
O50	U3	U1	94.15(16)	O13	C23	N15	119.3(8)
O50	U3	O32	89.1(2)	N15	C23	N14	114.1(8)
O50	U3	O2	88.0(2)	O12	C22	N14	129.0(8)
O50	U3	O1	93.6(2)	O12	C22	C11	116.7(6)
O50	U3	O31	90.6(2)	N14	C22	C11	114.2(7)

O50	U3	N31	84.8(2)	C25	C24	N15	93.2(11)
O2	U3	U2	38.35(12)	N12	C17	S11	122.9(7)
O2	U3	U1	99.79(12)	N13	C17	S11	121.9(7)
O2	U3	O32	137.85(17)	N13	C17	N12	114.9(9)
O2	U3	N31	159.14(18)	O11	C16	C15	115.3(7)
O1	U3	U2	33.44(13)	N12	C16	O11	128.8(8)
O1	U3	U1	28.03(13)	N12	C16	C15	115.8(8)
O1	U3	O32	66.47(18)	C19	C18	N13	112.8(11)
O1	U3	O2	71.76(18)	N13	C20	C21	113.5(10)
O1	U3	O31	166.47(18)	N31	C31	C42	114.8(7)
O1	U3	N31	128.16(18)	N31	C31	C32	122.6(7)
O31	U3	U2	133.58(13)	C32	C31	C42	122.6(7)
O31	U3	U1	164.06(14)	C31	C32	C33	117.9(7)
O31	U3	O32	126.52(18)	C34	C33	C32	119.4(8)
O31	U3	O2	95.56(18)	C35	C34	C33	119.1(8)
O31	U3	N31	65.02(19)	N31	C35	C36	113.7(7)
N31	U3	U2	161.31(12)	N31	C35	C34	121.7(7)
N31	U3	U1	100.25(13)	C34	C35	C36	124.6(7)
U2	U1	U3	56.880(8)	N11	C11	C22	114.6(7)
O33	U1	U2	164.09(14)	N11	C11	C12	122.1(7)
O33	U1	U3	107.28(14)	C12	C11	C22	123.3(7)
O33	U1	O32	68.66(18)	C11	C12	C13	117.9(7)
O33	U1	O13	87.8(2)	C14	C13	C12	119.3(8)
O33	U1	O12	156.97(18)	C15	C14	C13	119.0(8)
O32	U1	U2	95.69(11)	N11	C15	C16	114.3(7)
O32	U1	U3	38.99(11)	N11	C15	C14	122.0(7)
O32	U1	O12	134.29(15)	C14	C15	C16	123.7(7)
O20	U1	U2	91.59(19)	C81	P1	C71	110.5(4)
O20	U1	U3	90.55(19)	C81	P1	C51	108.8(4)
O20	U1	O33	86.7(3)	C51	P1	C71	108.7(4)
O20	U1	O32	93.4(2)	C61	P1	C81	111.4(5)
O20	U1	O1	91.5(2)	C61	P1	C71	107.0(4)
O20	U1	O13	90.6(3)	C61	P1	C51	110.5(4)
O20	U1	O12	92.8(2)	C82	C81	P1	115.8(6)
O10	U1	U2	91.44(19)	C71	C76	C75	120.7(9)
O10	U1	U3	92.03(17)	C74	C75	C76	119.8(8)
O10	U1	O33	90.7(3)	C75	C74	C73	120.8(9)
O10	U1	O32	87.4(2)	C74	C73	C72	119.1(10)
O10	U1	O20	176.8(3)	C71	C72	C73	120.3(9)
O10	U1	O1	91.7(2)	C76	C71	P1	119.8(7)
O10	U1	O13	87.4(2)	C72	C71	P1	121.0(6)
O10	U1	O12	88.8(2)	C72	C71	C76	119.2(7)
O1	U1	U2	28.49(15)	C51	C56	C55	119.4(11)



O1	U1	U3	28.39(15)	C54	C55	C56	118.6(12)
O1	U1	O33	135.7(2)	C53	C54	C55	122.0(12)
O1	U1	O32	67.24(19)	C54	C53	C52	120.1(13)
O1	U1	O13	136.5(2)	C51	C52	C53	120.2(12)
O1	U1	O12	67.35(19)	C56	C51	P1	120.0(8)
O13	U1	U2	108.04(14)	C52	C51	P1	120.3(8)
O13	U1	U3	164.90(14)	C52	C51	C56	119.5(9)
O13	U1	O32	155.83(18)	C65	C66	C61	120.4(9)
O13	U1	O12	69.17(18)	C64	C65	C66	121.8(10)
O12	U1	U2	38.88(11)	C65	C64	C63	118.1(11)
O12	U1	U3	95.74(11)	C64	C63	C62	121.9(10)
C43	O33	U1	135.6(6)	C63	C62	C61	118.4(9)
U1	O32	U3	102.45(18)	C66	C61	P1	119.7(7)
C42	O32	U3	126.1(4)	C66	C61	C62	119.4(9)
C42	O32	U1	131.2(4)	C62	C61	P1	120.8(7)
U3	O2	U2	103.33(17)	C27	C26	N15	111.4(12)
C1	O2	U2	115.4(5)				

---

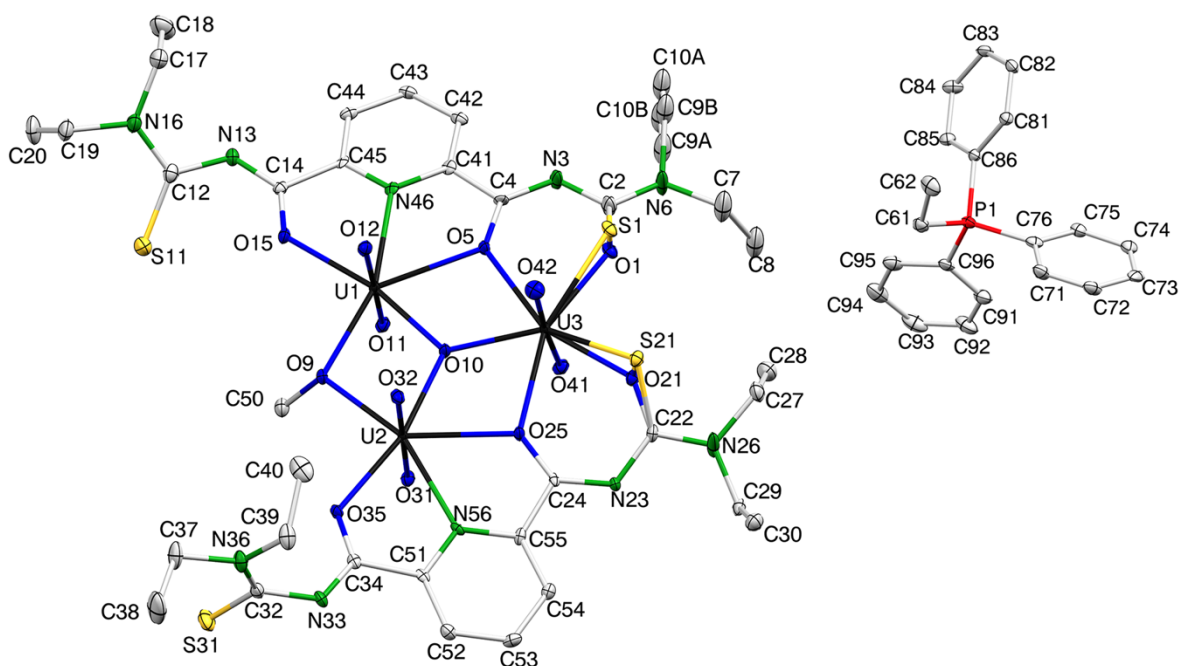


**Figure S4.** Ellipsoid representation of the complexes contained in the  $(\text{EtPPh}_3)[(\text{UO}_2)_3(\text{L}^{2\text{Et}_2})_2(\mu_2\text{-OMe})(\mu_3\text{-O})]_{0.9}/[(\text{UO}_2)_3(\text{L}^{\text{Et}_2})_2(\mu_2\text{-OMe})(\mu_3\text{-O})]_{0.1}$  mixed-crystals. The thermal ellipsoids are set at a 30% probability level. Hydrogen atoms are omitted for clarity.

**Table S8.** Bond lengths (Å) in  $(\text{EtPPh}_3)[(\text{UO}_2)_3(\text{L}^{2\text{Et}_2})_2(\mu_2\text{-OMe})(\mu_3\text{-O})]_{0.9}/[(\text{UO}_2)_3(\text{L}^{\text{Et}_2})_2(\mu_2\text{-OMe})(\mu_3\text{-O})]_{0.1}$ .

U3	U2	3.890(5)	C29	C30	1.518(8)
U3	U1	3.892(4)	S31	C32	1.675(6)
U3	O41	1.777(5)	C32	N33	1.391(7)
U3	O42	1.768(5)	C32	N36	1.332(8)
U3	O10	2.199(5)	N33	C34	1.286(7)
U3	O1	2.330(5)	C34	O35	1.283(7)
U3	S1	2.568(18)	C34	C51	1.501(8)
U3	O21	2.340(5)	N36	C37	1.463(8)
U3	S21	2.583(17)	N36	C39	1.479(8)
U3	O5	2.492(5)	C37	C38	1.495(10)
U3	O25	2.481(5)	C39	C40	1.504(10)
U2	U1	3.698(5)	C41	C42	1.385(8)
U2	O31	1.785(5)	C41	N46	1.339(7)
U2	O32	1.780(5)	C42	C43	1.387(8)
U2	O9	2.367(4)	C43	C44	1.383(8)
U2	O10	2.226(4)	C44	C45	1.390(8)
U2	O25	2.500(5)	C45	N46	1.335(7)
U2	O35	2.340(4)	C51	C52	1.378(8)
U2	N56	2.528(6)	C51	N56	1.335(7)
U1	O11	1.787(5)	C52	C53	1.389(8)

U1	O12	1.778(5)	C53	C54	1.383(8)
U1	O9	2.351(4)	C54	C55	1.371(8)
U1	O10	2.212(4)	C55	N56	1.348(7)
U1	O5	2.505(5)	P1	C61	1.793(6)
U1	O15	2.336(4)	P1	C76	1.789(7)
U1	N46	2.524(6)	P1	C86	1.791(6)
O9	C50	1.444(7)	P1	C96	1.786(7)
O1	S1	0.702(16)	C61	C62	1.523(9)
O1	C2	1.261(8)	C71	C72	1.376(9)
S1	C2	1.43(2)	C71	C76	1.396(9)
O21	S21	0.752(16)	C72	C73	1.380(10)
O21	C22	1.269(7)	C73	C74	1.382(10)
S21	C22	1.709(18)	C74	C75	1.370(9)
C2	N3	1.371(8)	C75	C76	1.379(9)
C2	N6	1.314(8)	C81	C82	1.386(9)
N3	C4	1.291(7)	C81	C86	1.382(8)
C4	O5	1.294(6)	C82	C83	1.375(9)
C4	C41	1.491(8)	C83	C84	1.379(9)
S11	C12	1.678(7)	C84	C85	1.381(9)
C12	N13	1.382(8)	C85	C86	1.387(9)
C12	N16	1.349(8)	C91	C92	1.383(10)
N13	C14	1.288(7)	C91	C96	1.385(9)
C14	O15	1.287(7)	C92	C93	1.362(11)
C14	C45	1.497(8)	C93	C94	1.374(11)
N16	C17	1.480(8)	C94	C95	1.393(10)
N16	C19	1.470(8)	C95	C96	1.387(9)
C17	C18	1.475(10)	N6	C7	1.479(9)
C19	C20	1.516(10)	N6	C9B	1.614(19)
C22	N23	1.373(7)	N6	C9A	1.570(18)
C22	N26	1.324(8)	C7	C8	1.463(12)
N23	C24	1.299(7)	C9B	C9A	1.32(3)
C24	O25	1.289(7)	C9B	C10B	1.52(3)
C24	C55	1.489(8)	C9B	C10A	0.701(18)
N26	C27	1.477(8)	C9A	C10B	0.837(19)
N26	C29	1.453(8)	C9A	C10A	1.49(3)
C27	C28	1.502(9)	C10B	C10A	1.27(2)

**Table S9.** Bond angles (°) in (EtPPh<sub>3</sub>)[(UO<sub>2</sub>)<sub>3</sub>(L<sup>2Et2</sup>)<sub>2</sub>(μ<sub>2</sub>-OMe)(μ<sub>3</sub>-O)]<sub>0.9</sub>/[(UO<sub>2</sub>)<sub>3</sub>(L<sup>Et2</sup>)<sub>2</sub>(μ<sub>2</sub>-OMe)(μ<sub>3</sub>-O)]<sub>0.1</sub>.

U2	U3	U1	56.74(10)	C22	O21	U3	136.1(4)
O41	U3	U2	92.71(15)	O21	S21	U3	63.0(13)
O41	U3	U1	93.11(14)	O21	S21	C22	43.2(11)

O41	U3	O10	91.82(18)	C22	S21	U3	101.6(8)
O41	U3	O1	84.87(19)	O1	C2	S1	29.5(7)
O41	U3	S1	100.4(4)	O1	C2	N3	125.7(6)
O41	U3	O21	88.86(18)	O1	C2	N6	119.3(6)
O41	U3	S21	105.0(4)	N3	C2	S1	121.8(9)
O41	U3	O5	89.65(16)	N6	C2	S1	116.1(9)
O41	U3	O25	86.57(16)	N6	C2	N3	114.8(5)
O42	U3	U2	90.64(16)	C4	N3	C2	122.2(5)
O42	U3	U1	90.57(16)	N3	C4	O5	129.5(5)
O42	U3	O41	175.99(19)	N3	C4	C41	115.7(5)
O42	U3	O10	92.2(2)	O5	C4	C41	114.7(5)
O42	U3	O1	92.5(2)	U3	O5	U1	102.31(14)
O42	U3	S1	77.0(4)	C4	O5	U3	132.2(3)
O42	U3	O21	88.06(19)	C4	O5	U1	125.0(3)
O42	U3	S21	71.7(4)	N13	C12	S11	124.4(5)
O42	U3	O5	92.22(17)	N16	C12	S11	122.9(5)
O42	U3	O25	94.66(17)	N16	C12	N13	112.3(5)
O10	U3	U2	28.66(11)	C14	N13	C12	125.4(5)
O10	U3	U1	28.16(10)	N13	C14	C45	115.4(5)
O10	U3	O1	135.50(16)	O15	C14	N13	130.0(5)
O10	U3	S1	134.1(4)	O15	C14	C45	114.4(5)
O10	U3	O21	135.51(15)	C14	O15	U1	127.6(4)
O10	U3	S21	136.6(4)	C12	N16	C17	122.8(5)
O10	U3	O5	67.00(13)	C12	N16	C19	120.6(5)
O10	U3	O25	67.20(14)	C19	N16	C17	116.6(5)
O1	U3	U2	164.05(12)	C18	C17	N16	113.7(6)
O1	U3	U1	107.57(16)	N16	C19	C20	112.8(6)
O1	U3	S1	15.5(4)	O21	C22	S21	23.9(6)
O1	U3	O21	88.9(2)	O21	C22	N23	124.7(5)
O1	U3	S21	86.4(4)	O21	C22	N26	119.9(5)
O1	U3	O5	68.61(17)	N23	C22	S21	125.9(7)
O1	U3	O25	155.90(14)	N26	C22	S21	112.0(7)
S1	U3	U2	159.6(4)	N26	C22	N23	115.3(5)
S1	U3	U1	106.5(4)	C24	N23	C22	121.6(5)
S1	U3	S21	82.4(6)	N23	C24	C55	115.5(5)
O21	U3	U2	106.86(15)	O25	C24	N23	129.9(5)
O21	U3	U1	163.54(11)	O25	C24	C55	114.6(4)
O21	U3	S1	89.2(4)	U3	O25	U2	102.69(15)
O21	U3	S21	16.7(4)	C24	O25	U3	131.2(3)
O21	U3	O5	157.48(14)	C24	O25	U2	125.7(3)
O21	U3	O25	68.44(18)	C22	N26	C27	118.9(6)
S21	U3	U2	109.4(4)	C22	N26	C29	123.1(5)
S21	U3	U1	158.2(4)	C29	N26	C27	117.9(5)

O5	U3	U2	95.65(12)	N26	C27	C28	111.2(6)
O5	U3	U1	38.96(8)	N26	C29	C30	111.2(5)
O5	U3	S1	69.0(4)	N33	C32	S31	120.3(5)
O5	U3	S21	149.9(4)	N36	C32	S31	124.7(5)
O25	U3	U2	38.83(8)	N36	C32	N33	114.7(5)
O25	U3	U1	95.35(13)	C34	N33	C32	121.5(5)
O25	U3	S1	156.5(4)	N33	C34	C51	115.8(5)
O25	U3	S21	74.1(4)	O35	C34	N33	128.3(5)
O25	U3	O5	133.88(15)	O35	C34	C51	115.9(5)
U1	U2	U3	61.66(4)	C34	O35	U2	126.0(3)
O31	U2	U3	94.88(15)	C32	N36	C37	122.5(5)
O31	U2	U1	92.06(12)	C32	N36	C39	122.1(5)
O31	U2	O9	87.41(16)	C37	N36	C39	115.3(5)
O31	U2	O10	92.70(17)	N36	C37	C38	111.3(6)
O31	U2	O25	89.71(18)	N36	C39	C40	111.6(5)
O31	U2	O35	91.01(17)	C42	C41	C4	122.2(5)
O31	U2	N56	84.58(16)	N46	C41	C4	115.3(5)
O32	U2	U3	86.67(15)	N46	C41	C42	122.5(5)
O32	U2	U1	90.74(12)	C41	C42	C43	118.0(5)
O32	U2	O31	177.19(17)	C44	C43	C42	119.6(5)
O32	U2	O9	94.65(16)	C43	C44	C45	118.7(5)
O32	U2	O10	89.78(17)	C44	C45	C14	123.7(5)
O32	U2	O25	90.05(18)	N46	C45	C14	114.7(5)
O32	U2	O35	86.88(17)	N46	C45	C44	121.6(5)
O32	U2	N56	92.83(16)	C41	N46	U1	122.0(4)
O9	U2	U3	99.88(13)	C45	N46	U1	118.1(4)
O9	U2	U1	38.25(11)	C45	N46	C41	119.4(5)
O9	U2	O25	137.79(12)	C52	C51	C34	123.9(5)
O9	U2	N56	158.86(13)	N56	C51	C34	113.9(5)
O10	U2	U3	28.27(9)	N56	C51	C52	122.2(5)
O10	U2	U1	33.45(10)	C51	C52	C53	118.6(5)
O10	U2	O9	71.62(17)	C54	C53	C52	119.1(5)
O10	U2	O25	66.47(15)	C55	C54	C53	119.1(5)
O10	U2	O35	166.69(13)	C54	C55	C24	123.9(5)
O10	U2	N56	128.21(16)	N56	C55	C24	114.3(5)
O25	U2	U3	38.48(11)	N56	C55	C54	121.8(5)
O25	U2	U1	99.91(9)	C51	N56	U2	118.1(4)
O25	U2	N56	61.81(13)	C51	N56	C55	119.2(5)
O35	U2	U3	163.47(9)	C55	N56	U2	122.1(3)
O35	U2	U1	133.64(10)	C76	P1	C61	111.4(3)
O35	U2	O9	95.80(17)	C76	P1	C86	107.1(3)
O35	U2	O25	126.36(15)	C86	P1	C61	110.8(3)
O35	U2	N56	64.89(15)	C96	P1	C61	109.2(3)

N56	U2	U3	100.27(12)	C96	P1	C76	110.1(3)
N56	U2	U1	161.34(10)	C96	P1	C86	108.2(3)
U2	U1	U3	61.60(6)	C62	C61	P1	115.7(5)
O11	U1	U3	92.43(14)	C72	C71	C76	119.6(6)
O11	U1	U2	91.78(12)	C71	C72	C73	120.2(6)
O11	U1	O9	88.80(17)	C72	C73	C74	120.3(6)
O11	U1	O10	91.01(17)	C75	C74	C73	119.6(6)
O11	U1	O5	89.44(18)	C74	C75	C76	120.8(6)
O11	U1	O15	91.50(17)	C71	C76	P1	121.0(5)
O11	U1	N46	83.86(16)	C75	C76	P1	119.4(5)
O12	U1	U3	89.08(14)	C75	C76	C71	119.5(6)
O12	U1	U2	90.11(12)	C86	C81	C82	120.8(6)
O12	U1	O11	177.99(17)	C83	C82	C81	119.0(6)
O12	U1	O9	92.25(16)	C82	C83	C84	121.1(6)
O12	U1	O10	90.95(16)	C83	C84	C85	119.7(6)
O12	U1	O5	90.90(18)	C84	C85	C86	120.1(6)
O12	U1	O15	86.70(17)	C81	C86	P1	119.0(5)
O12	U1	N46	94.54(16)	C81	C86	C85	119.3(6)
O9	U1	U3	100.12(14)	C85	C86	P1	121.7(5)
O9	U1	U2	38.54(10)	C92	C91	C96	119.9(7)
O9	U1	O5	138.66(13)	C93	C92	C91	120.4(7)
O9	U1	N46	157.77(14)	C92	C93	C94	120.4(7)
O10	U1	U3	27.97(9)	C93	C94	C95	120.2(7)
O10	U1	U2	33.69(11)	C96	C95	C94	119.3(7)
O10	U1	O9	72.16(17)	C91	C96	P1	120.1(5)
O10	U1	O5	66.58(14)	C91	C96	C95	119.7(6)
O10	U1	O15	166.97(13)	C95	C96	P1	120.1(5)
O10	U1	N46	128.76(16)	C2	N6	C7	121.8(6)
O5	U1	U3	38.72(10)	C2	N6	C9B	118.3(8)
O5	U1	U2	100.28(8)	C2	N6	C9A	118.8(8)
O5	U1	N46	62.43(13)	C7	N6	C9B	111.5(8)
O15	U1	U3	164.34(9)	C7	N6	C9A	116.0(7)
O15	U1	U2	133.41(11)	C9A	N6	C9B	48.9(9)
O15	U1	O9	95.11(17)	N6	C7	C8	111.4(7)
O15	U1	O5	126.22(14)	C9A	C9B	N6	63.8(12)
O15	U1	N46	64.25(17)	C9A	C9B	C10B	33.4(10)
N46	U1	U3	101.13(14)	C10B	C9B	N6	97.1(15)
N46	U1	U2	162.09(10)	C10A	C9B	N6	153(3)
U1	O9	U2	103.21(18)	C10A	C9B	C9A	90(3)
C50	O9	U2	118.0(3)	C10A	C9B	C10B	56(2)
C50	O9	U1	116.0(3)	C9B	C9A	N6	67.3(12)
U3	O10	U2	123.07(18)	C9B	C9A	C10A	28.0(9)
U3	O10	U1	123.87(17)	C10B	C9A	N6	153(3)

U1	O10	U2	112.86(19)	C10B	C9A	C9B	86(2)
S1	O1	U3	101.9(17)	C10B	C9A	C10A	58.3(19)
S1	O1	C2	88.5(17)	C10A	C9A	N6	95.1(14)
C2	O1	U3	140.3(4)	C9A	C10B	C9B	60.2(19)
O1	S1	U3	62.6(15)	C9A	C10B	C10A	88(2)
O1	S1	C2	62.0(15)	C10A	C10B	C9B	27.4(10)
C2	S1	U3	113.4(10)	C9B	C10A	C9A	62(3)
S21	O21	U3	100.3(14)	C9B	C10A	C10B	96(3)
S21	O21	C22	112.9(15)	C10B	C10A	C9A	34.1(10)

---

IR Spectrum (Wavenumber vs. Transmittance) showing characteristic absorption bands. The x-axis represents Wavenumber (cm⁻¹) from 4000 to 400, and the y-axis represents Transmittance (%T) from 7.5 to 52.5. The spectrum shows a broad peak around 3400 cm⁻¹ and several sharp peaks in the fingerprint region.

Wavenumber (cm⁻¹)	Transmittance (%T)
2974.23	~25
2831.80	~25
2682.89	~35
1498.69	~15
1425.40	~15
1379.10	~10
1249.87	~10
1101.35	~25
1010.70	~25
910.40	~10
785.74	~25
632.65	~25

24



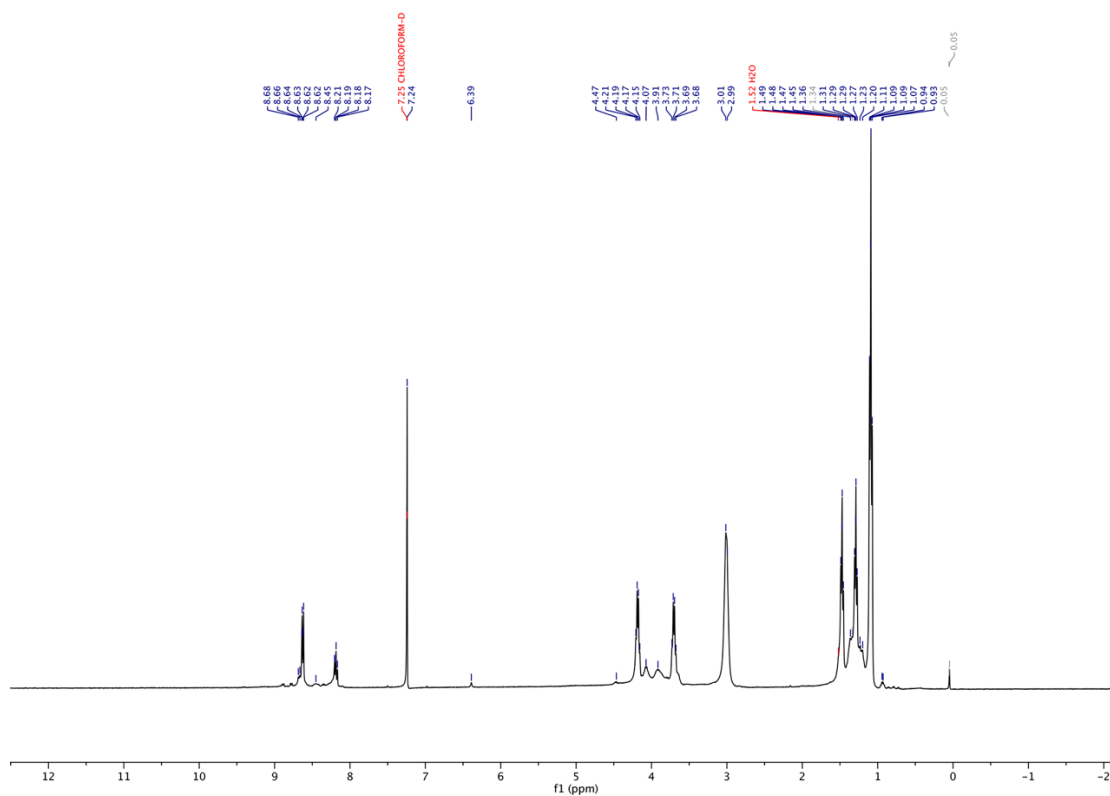


**Figure S7.**  $^1\text{H}$  NMR spectra of  $(\text{HNEt}_3)[(\text{UO}_2)_3(\text{L}^{2\text{Et}2})_2(\mu_2\text{-OH})(\mu_3\text{-O})]$ ,  $(\text{HNEt}_3)[9]$ , in  $\text{CDCl}_3$ .

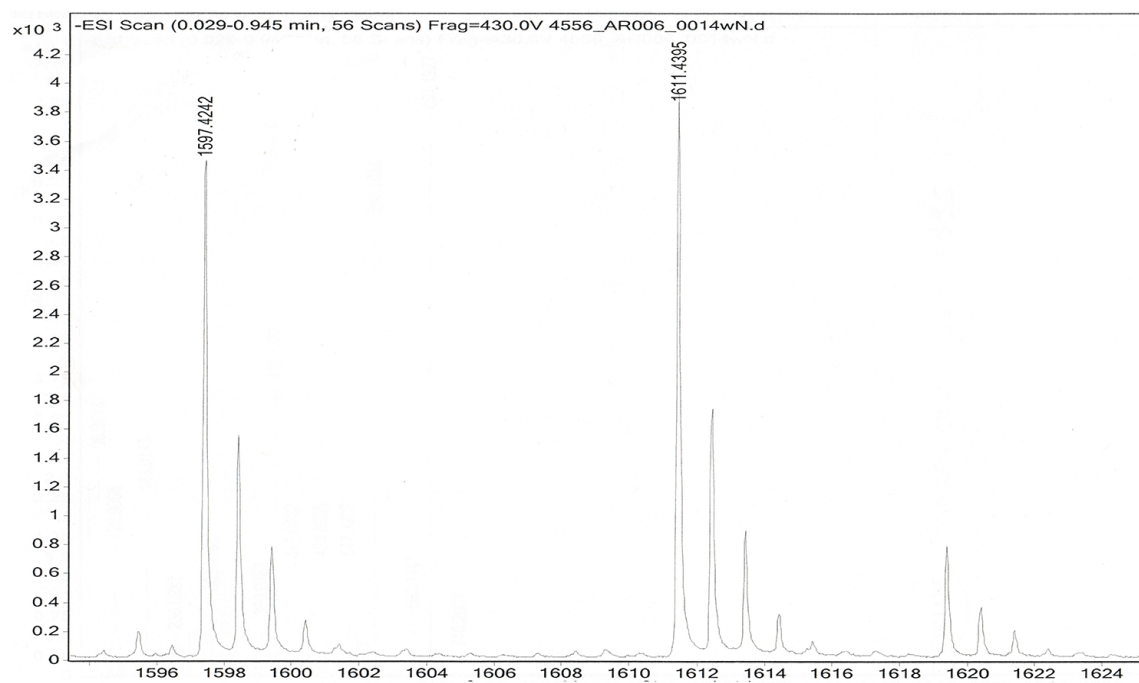


**Figure S8.** ESI(-) mass spectrum of  $(\text{HNEt}_3)[(\text{UO}_2)_3(\text{L}^{2\text{Et}2})_2(\mu_2\text{-OH})(\mu_3\text{-O})]$ ,  $(\text{HNEt}_3)[9]$ , in  $\text{CH}_2\text{Cl}_2$ .

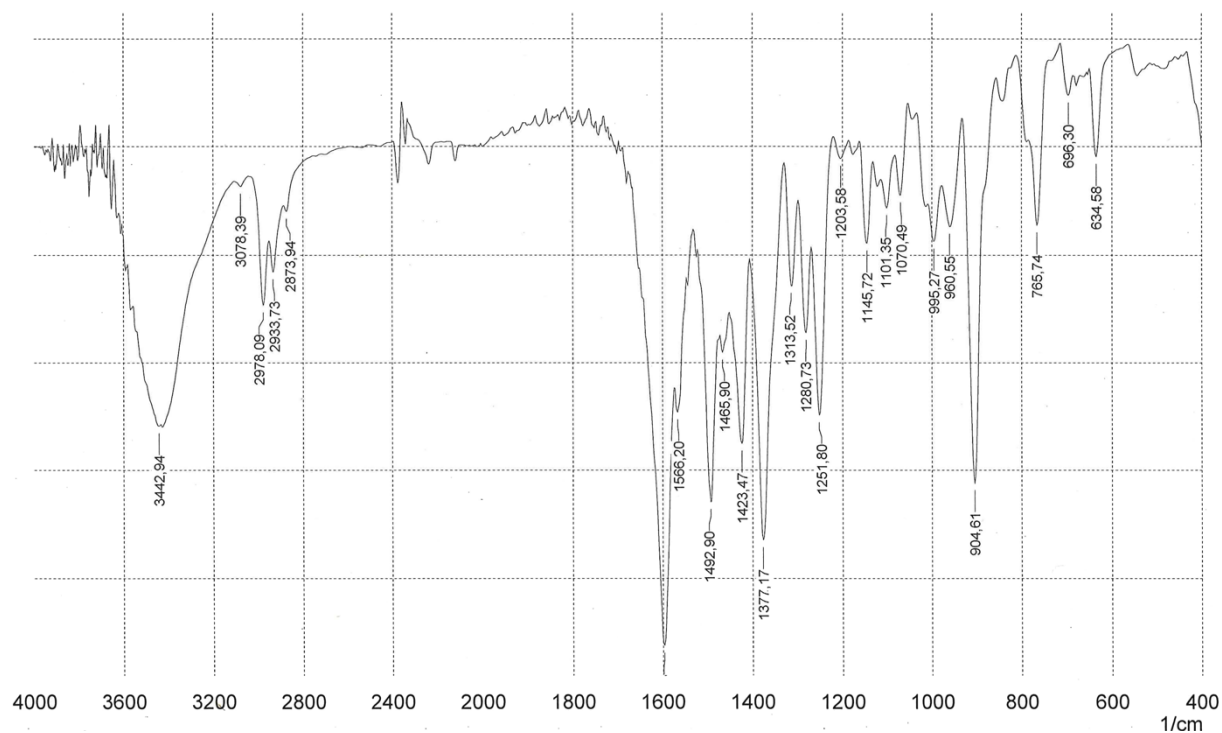


**Figure S9.** IR spectrum (KBr) of  $(\text{HNEt}_3)[(\text{UO}_2)_3(\text{L}^{2\text{Et}2})_2(\mu_2\text{-OEt})(\mu_3\text{-O})]$ ,  $(\text{HNEt}_3)[10]$ .

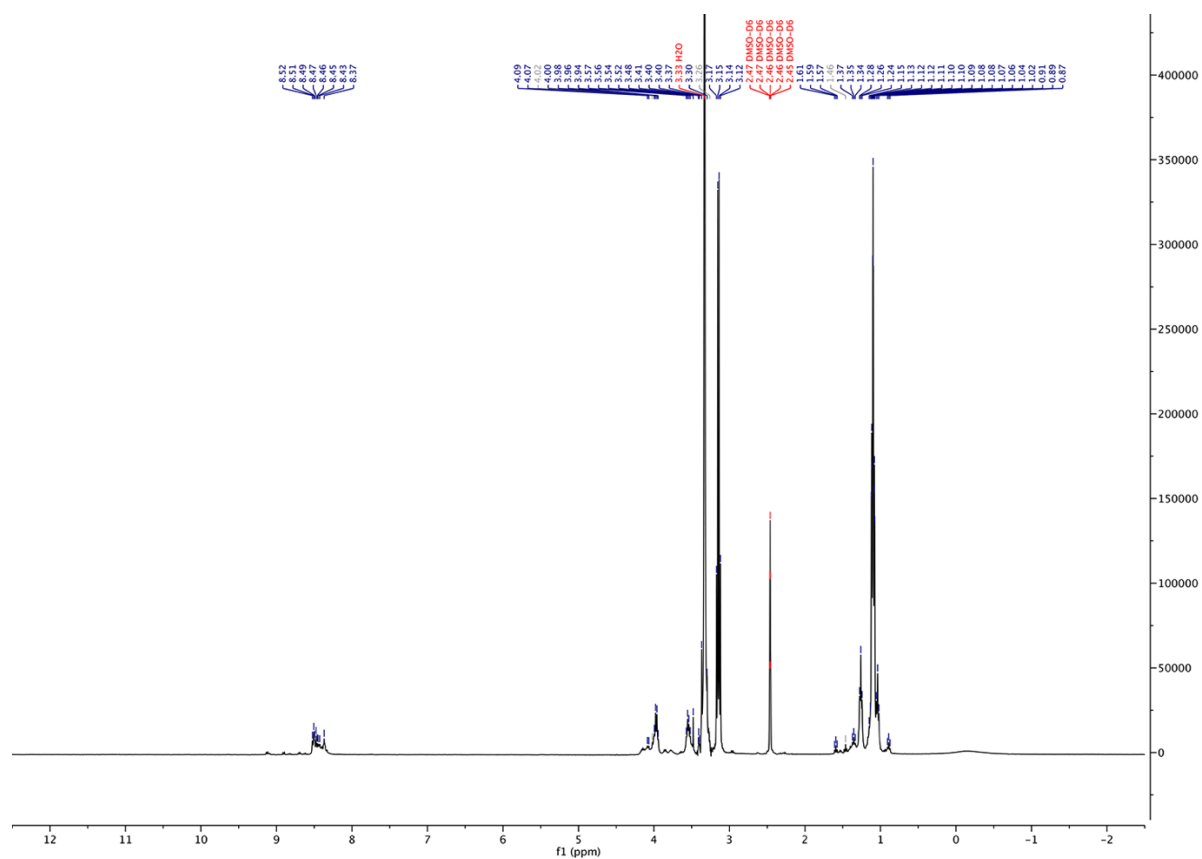


**Figure S10.**  $^1\text{H}$  NMR spectra of  $(\text{HNEt}_3)[(\text{UO}_2)_3(\text{L}^{2\text{Et}2})_2(\mu_2\text{-OEt})(\mu_3\text{-O})]$ ,  $(\text{HNEt}_3)[10]$ , in  $\text{DMSO-}D_6$ .

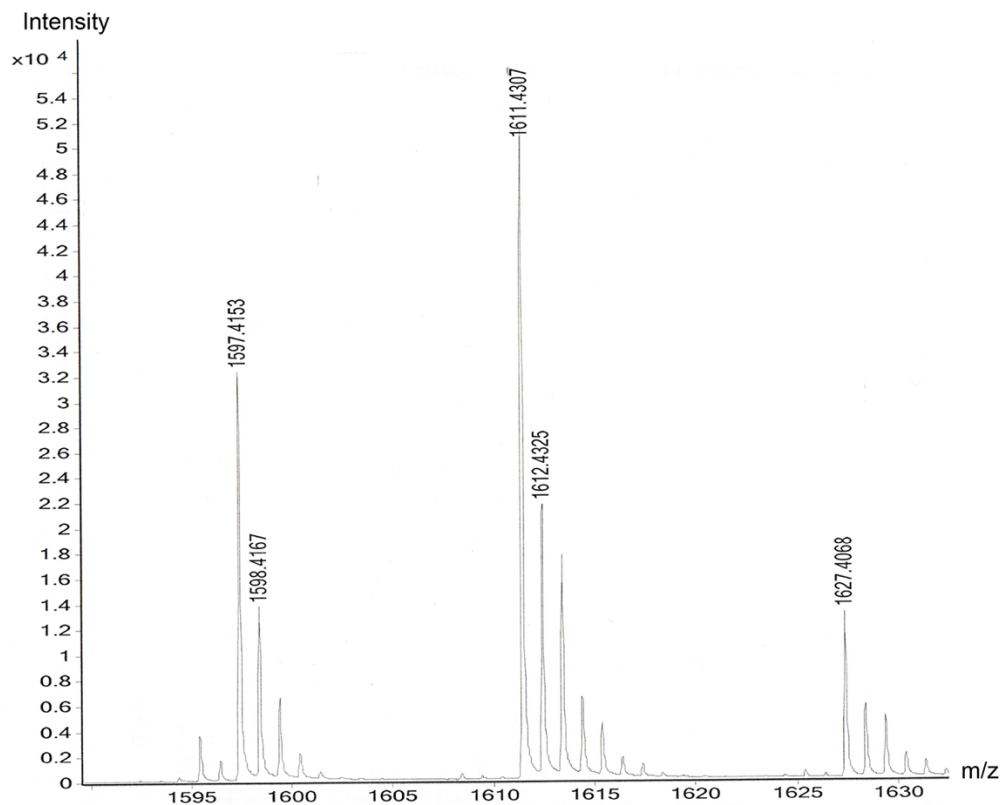


Figure S11. ESI(-) mass spectrum of  $(\text{HNEt}_3)[(\text{UO}_2)_3(\text{L}^{2\text{Et}_2})_2(\mu_2\text{-OEt})(\mu_3\text{-O})]$ ,  $(\text{HNEt}_3)[10]$ , in  $\text{CH}_2\text{Cl}_2$ .

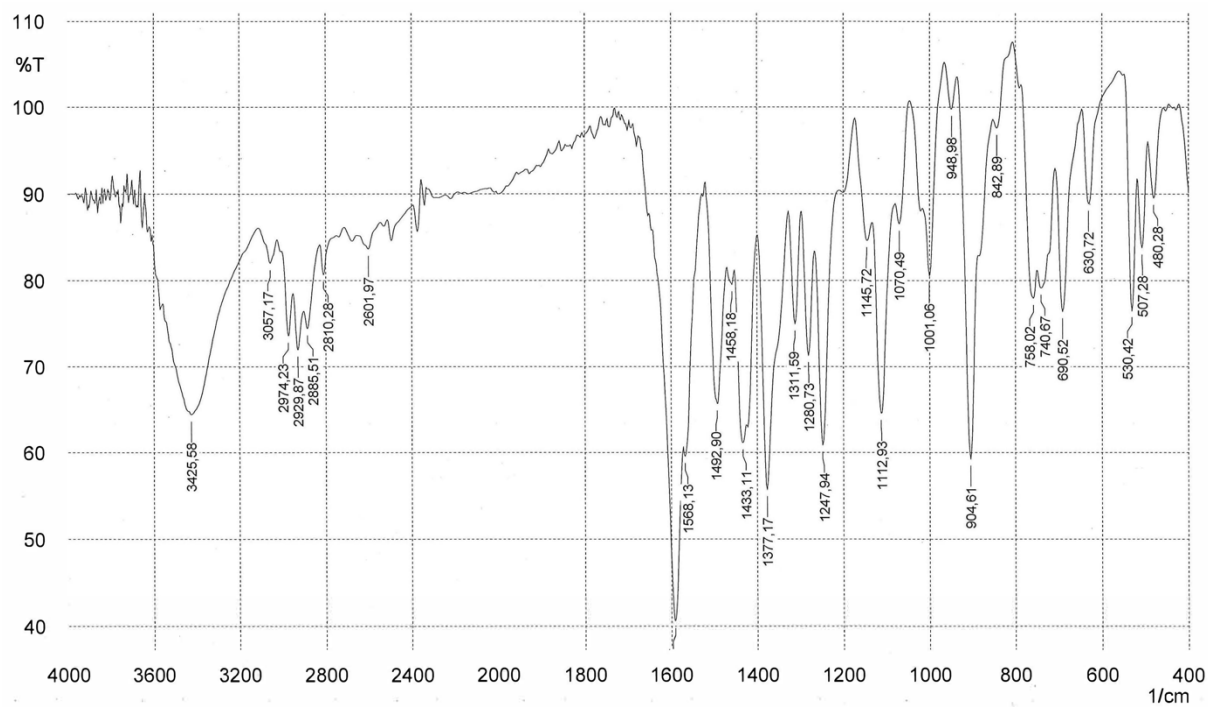
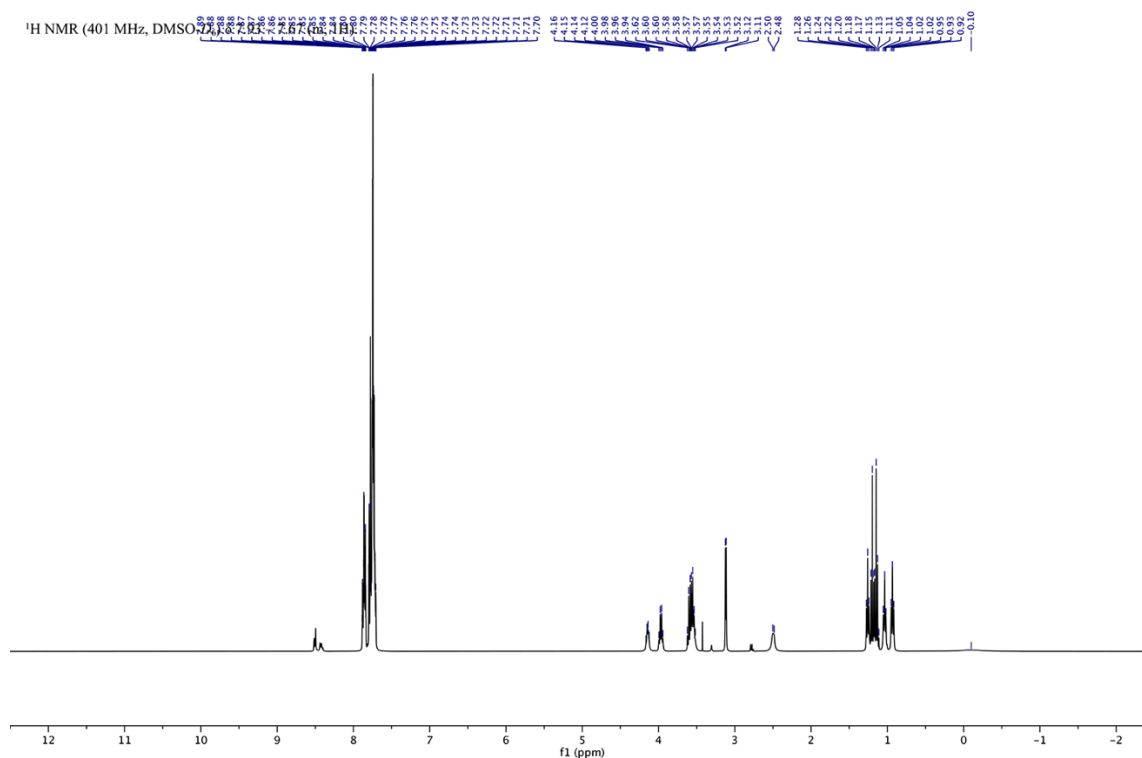


Figure S12. IR spectrum (KBr) of  $(\text{EtPPh}_3)[(\text{UO}_2)_3(\text{L}^{2\text{Et}_2})_2(\mu_2\text{-OMe})(\mu_3\text{-O})]$ ,  $(\text{EtPPh}_3)[11]$ .



**Figure S13.**  $^1\text{H}$  NMR spectra of  $(\text{EtPPh}_3)[(\text{UO}_2)_3(\text{L}^{2\text{Et}2})(\mu_2\text{-OMe})(\mu_3\text{-O})]$ ,  $(\text{EtPPh}_3)[11]$ , in  $\text{DMSO-D}_6$ .

### 3. Computational Chemistry

DFT (Density Functional Theory) calculations were performed with the high-performance computing system of the ZEDAT [78] using the program package GAUSSIAN 16 [79]. The gas phase geometry optimizations were performed using coordinates derived from the X-ray crystal structures. Calculations were performed using the hybrid density functional B3LYP [80–82] together with the 6-311G basis set for all atoms as implemented in Gaussian [83,84]. For initial optimization of uranium-containing compounds, the LANL2DZ basis set and the corresponding effective core potential (ECP) was used for uranium [85], while 6-311G was initially kept for the other atoms. The bigger 6-311++G\*\* basis set was used for the other atoms to obtain more reliable geometries [83,84,86–88]. Relativistic, dispersion corrected, all-electron calculations on the PBE0-DKH2-GD3BJ/SARC-DKH2(uranium)+aug-cc-pVTZ-DK(others) level as suggested in ref. [89] were attempted but the system size proved prohibitive. For comparable accuracy as outlined in ref. [90], calculations using the PBE0 hybrid functional ([91]) with Grimme dispersion and Becke-Johnson damping ([92]) using the Stuttgart relativistic large core ECP for uranium [93,94], and the def2-TZVPPD basis set for all other atoms [95,96] were attempted on the oxygen- and sulfur-bound isomers of  $[(\text{UO}_2)_3(\text{L}^{2\text{Et}2})_2(\mu_2\text{-OH})(\mu_3\text{-O})]^-$  to verify the reliability of conclusions derived from the B3LYP thermochemistry. The thermochemistry of the hypothetical, step-wise hydrolysis of the free ligand  $\{\text{L}^{\text{Et}2}\}^{2-}$  to give  $\{\text{L}^{2\text{Et}2}\}^{2-}$  was calculated on the same level as the uranium complexes to ensure comparability of the results (using the 6-311++G\*\* basis set [83,84,86–88] in frequency calculations based on the geometries obtained at 6-311G level that have been reported before in ref [43]). All basis sets were obtained from the EMSL database or the Basis Set Exchange repository [93,94]. Frequency calculations after the optimizations confirmed the convergence through the absence of imaginary frequencies.

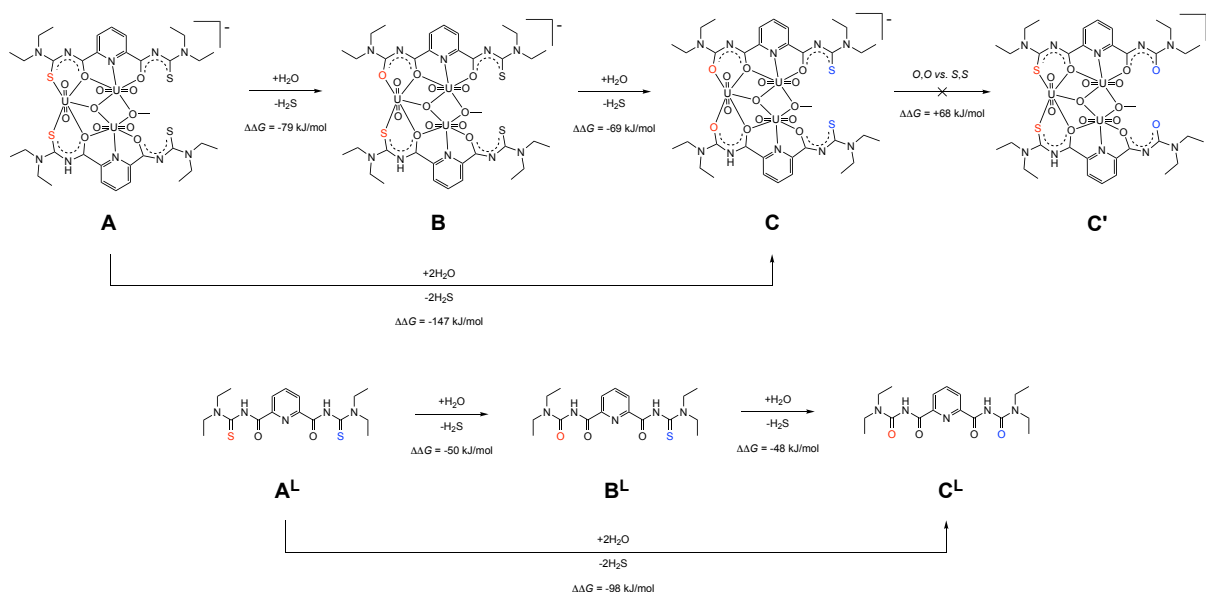


**Figure S14.** Considered hydrolysis reactions of trimetallic uranium complexes and the corresponding uncoordinated pro-ligands. Relative free energy differences for reactions and the hypothetical isomerization from O,O coordination in **C** to S,S coordination in **C'** are provided in SI units (gas-phase, standard conditions, B3LYP/LANL2DZ(uranium)+6-311++G\*\* (others) level). Geometries for the ligand structures were optimized at the B3LYP/6-311G level.

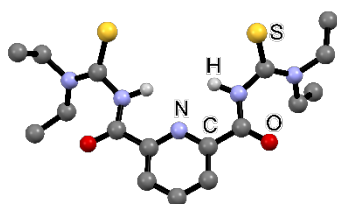


**Figure S15.** DFT optimized structure of **A<sup>L</sup>** (see Fig. S14). Hydrogen atoms bonded to carbon atoms are omitted for clarity. B3LYP/6-311G level. Taken from ref [42].

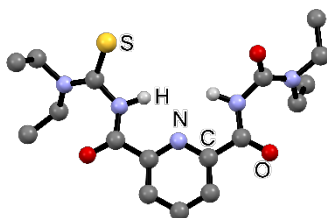


**Figure S16.** DFT optimized structure of **B<sup>L</sup>** (see Fig. S14). Hydrogen atoms bonded to carbon atoms are omitted for clarity. B3LYP/6-311G level.

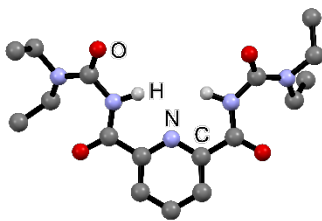


**Figure S17.** DFT optimized structure of C<sup>-</sup> (see Fig. S14). Hydrogen atoms bonded to carbon atoms are omitted for clarity. B3LYP/6-311G level.

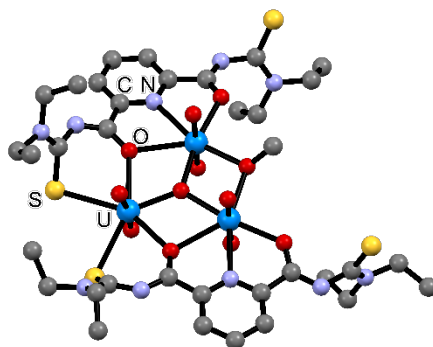


**Figure S18.** DFT optimized structure of A (see Fig. S14). Hydrogen atoms are omitted for clarity. B3LYP/LANL2DZ(uranium)+6-311++G\*\*(others) level.

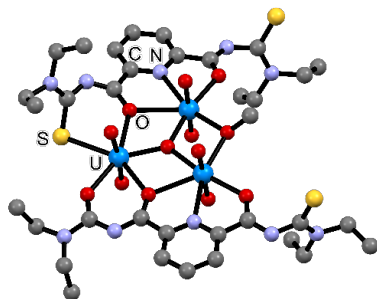


**Figure S19.** DFT optimized structure of B (see Fig. S14). Hydrogen atoms are omitted for clarity. B3LYP/LANL2DZ(uranium)+6-311++G\*\*(others) level.

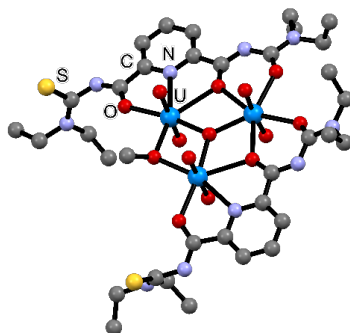


**Figure S20.** DFT optimized structure of C (see Fig. S14). Hydrogen atoms are omitted for clarity. B3LYP/LANL2DZ(uranium)+6-311++G\*\*(others) level.

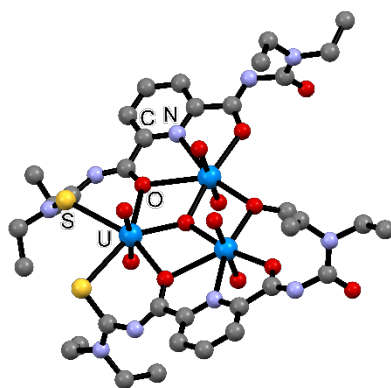


**Figure S21.** DFT optimized structure of **C'** (see Fig. S14). Hydrogen atoms are omitted for clarity. B3LYP/LANL2DZ(uranium)+6-311++G\*\*(others) level.

**Table S10.** Free energies  $\Delta G$  obtained by the DFT calculations (gas-phase, standard conditions, B3LYP/LANL2DZ(uranium)+6-311++G\*\*(others) level). Geometries for the ligand structures were optimized at the B3LYP/6-311G level.

		$\Delta G$	M + H <sub>2</sub> O	M + H <sub>2</sub> S
	H <sub>2</sub> S	-399.4272		
	H <sub>2</sub> O	-76.4549		
<b>Complex</b>	<b>A</b>	-4561.7161	-4638.1710	
	<b>B</b>	-4238.7737	-4315.2286	-4638.2010
	<b>C</b>	-3915.8275		-4315.2548
	<b>C'</b>	-3915.8016		
<b>Free ligand</b>	<b>A<sup>L</sup></b>	-1883.4918	-1959.9466	
	<b>B<sup>L</sup></b>	-1560.5386	-1636.9935	-1959.9658
	<b>C<sup>L</sup></b>	-1237.5847		-1637.0119

**Table S11.** Energies  $E$  obtained by the DFT calculations (gas-phase, top: PBE0-GD3BJ/StuttgartRLC(uranium)+def2-TZVPPD(others) level; bottom: B3LYP/LANL2DZ(uranium)+6-311++G\*\*(others) level).

	$E$ [Hartree]	$\Delta E$ [Hartree]	$\Delta E$ [kJ/mol]	$\Delta E$ [kcal/mol]
<b>C</b>	-3913.0848	0	0	0
	-3915.7027			
<b>C'</b>	-3913.0687	0.01614	42	10.1
	-3915.6777	0.02499	66	15.7

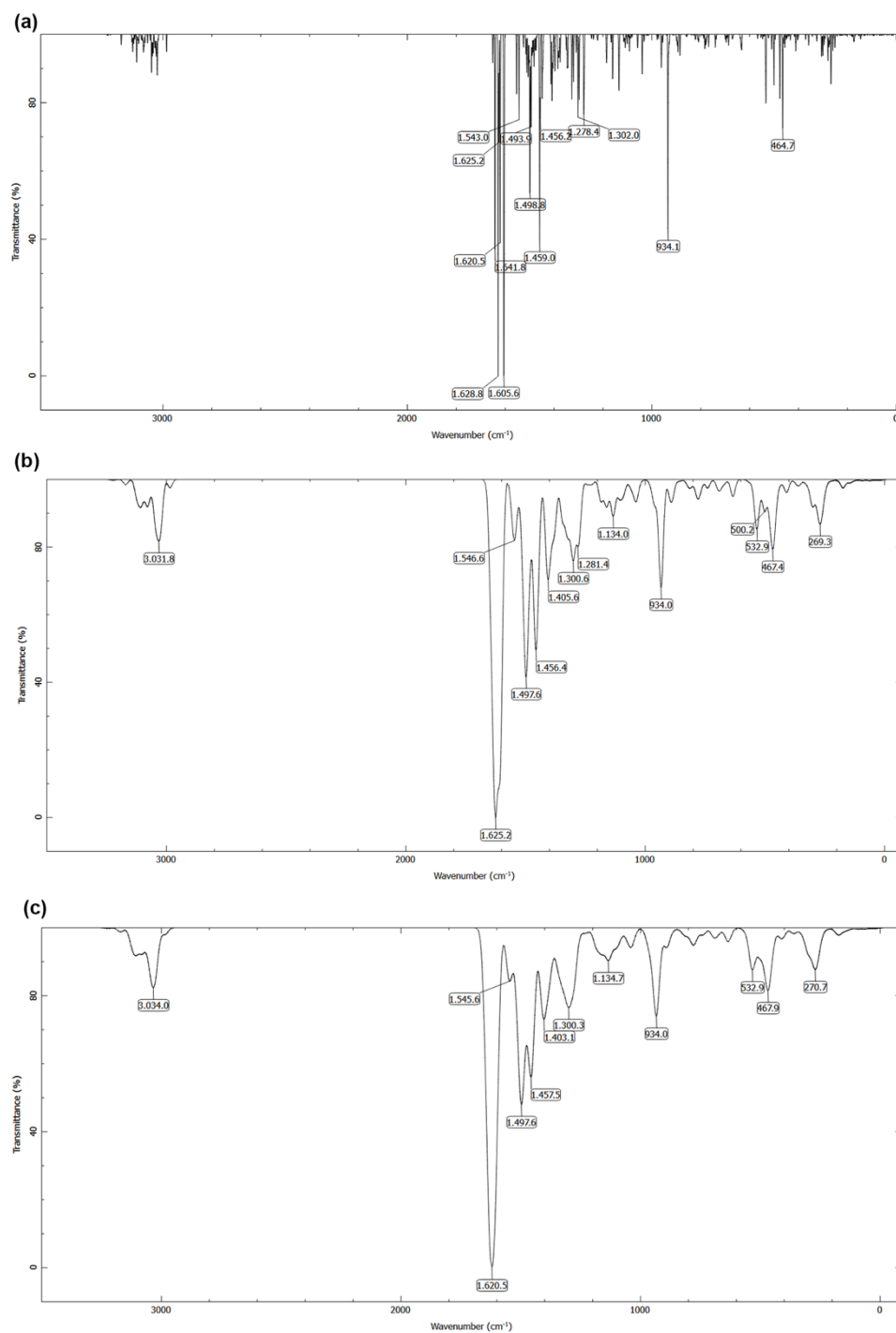


**Figure S22.** DFT-simulated IR frequencies for the  $[(\text{UO}_2)_3(\text{L}^{2\text{Et}2})_2(\mu_2\text{-OMe})(\mu_3\text{-O})]^-$  anion with spectral resolutions of (a) 2  $\text{cm}^{-1}$ , (b) 20  $\text{cm}^{-1}$  and (c) 30  $\text{cm}^{-1}$ . Note that no cation was included in the calculation. Despite the fact that the simulation has been conducted for the optimized gas phase structure, a good agreement is obtained with the frequencies in the experimental spectrum (see Fig. S12).



## 4. References

(Reference numbers are used in accordance with the respective numbers in the Article)

42. Noufele, C.N.; Hagenbach, A.; Abram, U. Uranyl Complexes with Aroylbis(*N,N*-dialkylthioureas). *Inorg. Chem.* **2018**, *57*, 12255–12269.
43. Noufele, C.N.; Schulze, D.; Roca Jungfer, M.; Hagenbach, A.; Abram, U. Bimetallic uranium complexes with 2,6-dipicolinoylbis(*N,N*-dialkylthioureas). *Molecules.* **2024**, *29*, 5001.
78. Bennett, L.; Melchers, B.; Proppe, B. High-Performance Computing at ZEDAT. Freie Universität, Berlin, Germany, 2020. Available online: <https://refubium.fu-berlin.de/handle/fub188/26993> (accessed on 24 October 2024).
79. Frisch, M.J.; Trucks, G.W.; Schlegel, H.B.; Scuseria, G.E.; Robb, M.A.; Cheeseman, J.R.; Scalmani, G.; Barone, V.; Petersson, G.A.; Nakatsuji, H.; et al. *Gaussian 16*, Revision A.03; Gaussian, Inc.: Wallingford, CT, USA, 2016.
80. Vosko, S.H.; Wilk, L.; Nusair, M. Accurate spin-dependent electron liquid correlation energies for local spin density calculations: A critical analysis. *Can. J. Phys.* **1980**, *58*, 1200–1211.
81. Becke, A.D. Density-functional thermochemistry. III. The role of exact exchange. *J. Chem. Phys.* **1993**, *98*, 5648–5652.
82. Lee, C.; Yang, W.; Parr, R.G. Development of the Colle-Salvetti correlation-energy formula into a functional of the electron density. *Phys. Rev. B* **1988**, *37*, 785–789.
83. Krishnan, R.; Binkley, J. S.; Seeger, R.; Pople, J. A. Self-consistent molecular orbital methods. XX. A basis set for correlated wave functions. *J. Chem. Phys.* **1980**, *72*, 650–654.
84. McLean, A. D., Chandler, G. S. Contracted Gaussian basis sets for molecular calculations. I. Second row atoms, *Z*=11–18. *J. Chem. Phys.* **1980**, *72*, 5639–5648.
85. Hay, P. J. Ab initio studies of excited states of polyatomic molecules including spin-orbit and multiplet effects: The electronic states of UF<sub>6</sub>. *J. Chem. Phys.* **1983**, *79*, 5469–5482.
86. Spitznagel, G. W., Clark, T., Schleyer, P. von Ragué, Hehre, W. J. An evaluation of the performance of diffuse function-augmented basis sets for second row elements, Na–Cl. *J. Comput. Chem.* **1987**, *8*, 1109–1116.
87. Clark, T., Chandrasekhar, J., Spitznagel, G. W., Schleyer, P. Von Ragué. Efficient diffuse function-augmented basis sets for anion calculations. III. The 3-21+G basis set for first-row elements, Li–F. *J. Comput. Chem.* **1983**, *4*, 294–301.
88. Francl, M. M., Pietro, W. J., Hehre, W. J., Binkley, J. S., Gordon, M. S., DeFrees, D. J., Pople, J. A. Self-consistent molecular orbital methods. XXIII. A polarization-type basis set for second-row elements. *J. Chem. Phys.* **1982**, *77*, 3654–3665.
89. Pantazis, D.A.; Neese, F. All-Electron Scalar Relativistic Basis Sets for the Actinides. *J. Chem. Theory Comput.* **2011**, *7*, 677–684.
90. Shamov, G.A.; Schreckenbach, G.; Vo, T. N. A Comparative Relativistic DFT and Ab Initio Study on the Structure and Thermodynamics of the Oxofluorides of Uranium(IV), (V) and (VI). *Chem. Eur. J.* **2007**, *13*, 4932–4947.
91. Adamo, C., Barone, V. Toward reliable density functional methods without adjustable parameters: The PBE0 model. *J. Chem. Phys.* **1999**, *110*, 6158–6170.
92. Grimme, S., Ehrlich, S., Goerigk, L. Effect of the damping function in dispersion corrected density functional theory, *J. Comp. Chem.* **2011**, *32*, 1456–1465.
93. Feller, D. The role of databases in support of computational chemistry calculations. *J. Comput. Chem.* **1996**, *17*, 1571–1586.
94. Schuchardt, K.L.; Didier, B.T.; Elsethagen, T.; Sun, L.; Gurumoorthi, V.; Chase, J.; Li, J.; Windus, T.L. Basis Set Exchange: A Community Database for Computational Sciences. *J. Chem. Inf. Model.* **2007**, *47*, 1045–1052.
95. Rappoport, D., Furche, F. Property-optimized Gaussian basis sets for molecular response calculations. *J. Chem. Phys.* **2010**, *133*, 134105.
96. Weigend, F., Ahlrichs, R. Balanced basis sets of split valence, triple zeta valence and quadruple zeta valence quality for H to Rn: Design and assessment of accuracy. *Phys. Chem. Chem. Phys.* **2005**, *7*, 3297.